

**Determination of stoichiometric parameters in
respirometric tests from full-scale operating HSSF
constructed wetlands**

Akram Abdel Khalek Sayed

Dissertation of the Master in
Environmental Engineering

Supervisors: Prof. Ana Fonseca Galvão, Prof. dr. ir. Diederik Rousseau

Assistant supervisor: Eng. Joana PISOEIRO

Examination Committee

Chairperson: Maria Joana Castelo-Branco de Assis Teixeira Neiva Correia

Supervisor: Prof. dr. ir. Diederik Rosseau

Members of Committee: Helena Maria Rodrigues Vasconcelos Pinheiro

June 2019

I declare that this document is an original work of my own authorship and that it fulfils
all the requirements of the Code of Conduct and Good Practices of the
Universidade de Lisboa.

Acknowledgements

First of all, I would like to thank my supervisor professor Ana Galvão to welcome me at Técnico and to make me feel at home. Besides that, it is truly remarkable how dedicated you are with your work and everyone around it. All your students get the best guidance and help, despite the loads of work you have. So thank you again for the support!

Everyone who recently worked with professor Galvão will know Joana Piseiro as the right hand of the professor. I've had a lot of help with practical issues in the lab and with the calculation methods which I'm really grateful for. Next to the work you were always around to cheer everyone up in the lab or to check if we were still fine. I've had answers for all the questions I've asked, regardless the time. Therefore I would say 'muito obrigado' to both my Portuguese supervisors.

Together with the mentors from Técnico, I would like to thank my Belgian supervisor Prof. dr. ir. Diederik Rousseau. Thank you for pushing me to deliver a script of the highest quality, your quick responses and to motivate me to continuously work hard.

Of course I have to mention my parents, the two most important people who've supported me daily with all they have. At difficult moments, they always had a solution to lighten the work. Even when I was abroad they managed to help me with their best advice. They gave me all the opportunities I needed, and I hope I can make them proud with what I've achieved today.

It wouldn't be fair not to mention my girlfriend. Being away from each other for so long is never easy. Nevertheless I always had the support and never-ending love I needed. So thank you for bearing all my complaining. Even though you're not familiar with the work I do, you always listened carefully to my problems or explanations and tried to help me as much as possible.

At last I would like to thank all my friends for their friendship and encouragement. Everyone had their special way to keep me motivated.

Abstract

This research studies microorganisms' activity in biofilms from a horizontal subsurface flow constructed wetland (HSSF-CW) treating municipal wastewater. It thereby transposes lab-scale work to a full-scale operating HSSF-CW with soil media and *Phragmites australis*. Ten samples across the wetland were collected to determine heterotrophic growth yield coefficients (Y_H and Y_{STO}). The aim is to establish a better understanding of the internal processes and to develop stoichiometric parameters for modelling.

Samples, manually obtained, were placed inside an LSF-respirometer (Liquid phase, Static gas, Flowing liquid) for testing aerobic substrate biodegradation. The respirometer includes a closed box with the sample wedged between two vertical gravel layers. During the tests DO-concentrations of recirculating water from an aerated tank placed before the inlet are measured together with those of the outlet of the box. Tracer tests were used to determine the hydraulic retention time (HRT) and volatile attached solids (VAS) were measured to obtain the biomass in each sample. Most of the respirograms (12) obtained had a peak value followed by a decrease in OUR. Seven profiles revealed slower reactions to substrate additions. Six results, corresponding to the inlet and outlet of the wetland, had a plateau of maximum OUR. Average results for Y_H were measured as 0.852 mgCOD/mgCOD and for Y_{STO} as 0.895 mgCOD/mgCOD, with ranges of 0.324-0.961 and 0.794-0.968 mgCOD/mgCOD respectively. Extremely fluctuating results were observed. Based on the HRT and VAS a potential preferential flow path is assumed at the right-hand side of the CW with a clogged area at the centre.

Keywords: Constructed wetland; respirometry; growth yield; storage mechanism; OUR-profile.

Resumo

O presente trabalho analisa a actividade microbiana de biofilmes presentes em leitos de macrófitas de escoamento sub-superficial horizontal (LM-SSH) de uma Estação de Tratamento de Águas Residuais. O leito analisado tem solo como meio de enchimento e está plantado com *Phragmites australis*. Foram recolhidas amostras de dez pontos distribuídos pelo leito destinadas a determinar valores de rendimento de crescimento heterotrófico, incluindo para a condição de armazenamento de substrato (Y_H e Y_{STO}), para futura utilização em estudos de modelação.

As amostras foram colocadas dentro de um respirómetro LSF (fase líquida, gás estático, líquido circulante) que permite acompanhar a biodegradação aeróbia de um substrato. Durante os testes, são medidas as concentrações de oxigénio dissolvido da água que recircula entre um tanque arejado, colocado antes da entrada da caixa que contém a amostra, e a saída da caixa. Foi utilizado um teste de traçador para determinar o tempo de retenção hidráulica (TRH) e os sólidos voláteis (SV) foram medidos para obter a biomassa.

Foram obtidos 12 perfis com um pico inicial seguido de decréscimo de consumo de oxigénio (OUR), e 7 perfis apresentaram uma resposta inicial à adição de substrato mais lenta. Apenas 6 dos respirogramas, correspondentes à entrada e saída do leito, apresentaram um patamar de OUR máximo. Os resultados apresentaram uma variação elevada, tendo-se obtido valores médios para Y_H de 0,776 mgCOD/mgCOD e para Y_{STO} de 0,895 mgCOD/mgCOD. Baseado no THR e SV, foi identificado um potencial caminho preferencial no lado direito do leito com uma área colmatada no centro.

Palavras-chave: Leito de macrófitas; respirometria; rendimento de crescimento; mecanismos de armazenamento; perfil de consumo de oxigénio.

Samenvatting

Dit onderzoek zal de activiteit bestuderen van micro-organismen in biofilms uit een rietveld met een horizontale, ondergrondse stroming (HSSF-CW) die gemeentelijk afvalwater behandelt. Hierbij wordt het werk op laboschaal verplaatst naar een HSSF-CW werkzaam op volledige schaal met bodem als vulmedium en *Phragmites australis* als vegetatie. Tien stalen uit verschillende punten op het rietveld werden verzameld om de coëfficiënten voor de heterotrofe groeiopbrengst te bepalen (Y_H en Y_{STO}). Het doel omvat hierbij het verwerven van een beter inzicht in de inwendige processen van het rietveld en om stoichiometrische parameters te voorzien die kunnen helpen in het modelleren.

De stalen, manueel verzameld, werden in een LSF-respirometer geplaatst (Vloeistoffase, Statisch gas, Vloeiend vloeistof) die geschikt is om aerobe substraatbiodegradatie te meten. De respirometer bestaat uit een gesloten doos met de stalen geplaatst tussenin twee verticale gravel-lagen. Tijdens de testen werden de zuurstofconcentraties gemeten van het recirculerende water uit een beluchte tank voor de ingang, tezamen met de zuurstof van het water aan de uitgang van de doos. Een tracertest werd uitgevoerd om de hydraulische verblijftijd (HRT) te meten en vluchtige aangehechte vaste delen (VAS) werden bepaald om de biomassa in ieder staal te kennen.

Er werden voornamelijk respirogrammen (12) verkregen met een piek gevolgd door een daling in OUR en 7 profielen toonden tragere reacties na toevoegen van substraat. Enkel 6 respirogrammen, overeenstemmend met de ingang en uitgang van het rietveld, bevatten een plateau met een maximale OUR. Het gemiddelde resultaat voor Y_H is 0.852 mg COD/mg COD, voor Y_{STO} is dit 0.895 mg COD/mg COD. Door de extreem schommelende resultaten werden weinig tot geen correlaties waargenomen tussen de verschillende parameters. Gebaseerd op de HRT en VAS wordt er verondersteld dat een preferentiële stroom bestaat aan de rechterhandzijde van het rietveld, met een verstopte zone centraal in het bed.

Sleutelbegrippen: Rietveld; respirometrie; groeiopbrengst; opslagmechanisme; zuurstofopname snelheidsprofiel.

Table of contents

Acknowledgements	iii
Abstract.....	iv
Resumo	vi
Samenvatting.....	viii
Table of contents	x
List of tables	xii
List of figures	xii
List of abbreviations.....	xv
1. Introduction	1
1.1 Context and motivation.....	2
1.2 Thesis objectives and outline	2
2. State-of-the-art.....	4
2.1 Constructed wetlands	5
2.1.1 Overview.....	5
2.1.2 Horizontal subsurface flow wetlands	6
2.1.3 Clogging.....	8
2.1.4 Modelling tools for biodegradation.....	9
2.2 Respirometry	14
2.2.1 Principles	14
2.2.2 Respirometer	15
2.2.3 Respirogram	16
2.2.3.1 Characterization of the respirogram	16
2.2.3.2 Endogenous respiration.....	19
2.2.4 Interferences.....	20
2.2.4.1 Nitrification	20
2.2.4.2 Sulphur and iron bacteria	22
2.2.5 Process parameters	22
2.3 Calculations for the stoichiometric parameters	25

3.	Materials and methods	28
3.1	Investigated full-scale operating wetland: Barroca d'Alva	29
3.2	Sampling methodology	31
3.3	Respirometry test	32
3.3.1	Setup	32
3.3.1.1	LSF respirometer: box reactor	34
3.3.2	Preparation	35
3.3.3	Test procedure.....	37
3.4	Post-measuring	39
3.4.1	Tracer test and hydraulic retention time	39
3.4.2	Dry matter and volatile attached solids	40
4.	Results and discussion	42
4.1	Tracer tests and hydraulic retention time	43
4.2	Dry matter and volatile attached solids (biomass).....	46
4.3	Respirograms and yield coefficients.....	49
4.4	Summary of results and discussion.....	62
4.4.1	Summary of parameters and their correlation	62
4.4.2	Growth yields	65
4.4.3	Respirogram types.....	66
5.	Conclusion	68
5.1	Conclusion	69
5.2	Future research suggestions	71
	References	72
	Appendices	I
	Appendix A: SSAG stoichiometric- and kinetic parameters for respirometry	I
	Appendix B: Results for the constructed wetland influent and effluent concentrations	II
	Appendix C: HRT-profiles for every sample	III

List of tables

Table 1: ASM3 parameters (Henze et al., 2000).....	11
Table 2: ASM3 processes (Henze et al., 2000).....	11
Table 3: Constructed wetland influent and effluent concentrations (2006 - 2018).....	30
Table 4: Description of the operating procedure.....	37
Table 5: HRT and standard deviation of each sample.....	44
Table 6: Determined dry matter and volatile attached solids.....	47
Table 7: Summary of the stoichiometric results and F:M ratios.....	62
Table 8: Summary of results (2).....	64
Table 9: A summary of the stoichiometric- and kinetic parameters for respirometry according to the SSAG model (Hoque et al., 2008).....	I
Table 10: Constructed wetland influent and effluent concentrations (2002 - 2005).....	II

List of figures

Figure 1: Typical HSSF wetland (Tilley et al., 2014)	6
Figure 2: ASM1 subdivision of components (Jeppsson, 1996).....	10
Figure 3: Cell respiration	14
Figure 4: LSF-respirometer (Galvão, 2017)	16
Figure 5: Respirogram (Ortigara et al., 2011)	17
Figure 6: 3 different types of OUR profiles perceived in the study of PISOEIRO et al. (2017) ..	18
Figure 7: Respirogram with nitrification (Andreottola et al., 2007)	21
Figure 8: Schematic overview of the SSAG model (Hoque et al., 2008)	25
Figure 9: Calculations on the respirogram (PISOEIRO, 2018)	25
Figure 10: Location of the WWTP	29
Figure 11: Constructed wetlands Barroca D'Alva.....	29
Figure 12: Map of samples taken, with distances.	31
Figure 13: Sampling tube	32
Figure 14: Representation of the LSF respirometer test setup.....	33

Figure 15: Adjusted box reactor of the LSF respirometer. Grey areas are the tape used to secure the mesh.....	34
Figure 16: Inside view of the box of the LSF respirometer	35
Figure 17: Filled reactor of the LSF respirometer.....	35
Figure 18: Tracer test step response graph (Bonner et al., 2017).....	39
Figure 19: HRT profile for sample 1	43
Figure 20: 3D overview of the HRT (min) of each sample according to the wetland position	44
Figure 21: CW overview with the HRT (min) from each sample at the respirometer	45
Figure 22: 3D overview of the VAS (g/L) of each sample according to the wetland position .	48
Figure 23: Respirogram and stoichiometric results sample 1, test 1 (26/10/2018)	50
Figure 24: Respirogram and stoichiometric results sample 1, test 2 (29/10/2018)	50
Figure 25: Respirogram and stoichiometric results sample 1, test 3 (30/10/2018)	51
Figure 26: Respirogram and stoichiometric results sample 1, test 4 (31/10/2018)	51
Figure 27: Respirogram and stoichiometric results sample 2, test 1 (11/11/2018)	52
Figure 28: Respirogram and stoichiometric results sample 2, test 2 (13/11/2018)	52
Figure 29: Respirogram and stoichiometric results sample 2, test 3 (14/11/2018)	52
Figure 30: Respirogram and stoichiometric results sample 3, test 1 (18/11/2018)	53
Figure 31: Respirogram and stoichiometric results sample 3, test 2 (19/11/2018)	53
Figure 32: Respirogram and stoichiometric results sample 3, test 3 (20/11/2018)	54
Figure 33: Respirogram and stoichiometric results sample 3, test 4 (21/11/2018)	54
Figure 34: Respirogram and stoichiometric results sample 4, test 1 (6/12/2018)	55
Figure 35: Respirogram and stoichiometric results sample 4, test 2 (7/12/2018)	55
Figure 36: Respirogram and stoichiometric results sample 4, test 3 (9/12/2018)	55
Figure 37: Respirogram and stoichiometric results sample 4A, test 1 (2/12/2018).....	56
Figure 38: Respirogram and stoichiometric results sample 4A, test 2 (3/12/2018).....	57
Figure 39: Respirogram and stoichiometric results sample 4A, test 3 (3/12/2018).....	57
Figure 40: Respirogram and stoichiometric results sample 4A, test 4 (4/12/2018).....	57
Figure 41: Respirogram and stoichiometric results sample 6 (12/12/2018).....	58

Figure 42: Respirogram and stoichiometric results sample 7, test 1 (18/12/2018)	59
Figure 43: Respirogram and stoichiometric results sample 7, test 2 (18/12/2018)	59
Figure 44: Respirogram and stoichiometric results sample 7, test 3 (19/12/2018)	59
Figure 45: Respirogram and stoichiometric results sample 8, test 1 (17/01/2019)	60
Figure 46: Respirogram and stoichiometric results sample 8, test 2 (17/01/2019)	60
Figure 47: Respirogram and stoichiometric results sample 8, test 3 (18/01/2019)	61
Figure 48: Respirogram and stoichiometric results sample 9, test 1 (20/01/2019)	61

List of abbreviations

AMO	Ammonia monooxygenase
ASM	Activated sludge model
ATP	Adenosine triphosphate
BM	Biomass
BOD	Biochemical oxygen demand
COD	Chemical oxygen demand
CW	Constructed wetland
CWM	Constructed wetland model
DM	Dry matter
DO	Dissolved oxygen
F:M-ratio	Food to microorganisms ratio
FWS	Free water surface
HRT	Hydraulic retention time
HSSF	Horizontal subsurface flow
LSF	Liquid phase, Static gas, Flowing liquid
MO	Microorganisms
OUR	Oxygen uptake rate
RZM	Root-Zone Method
SSAG	Simultaneous storage and growth
TKN	Total Kjeldahl Nitrogen
VAS	Volatile attached solids
VBA	Visual basic for applications
VF	Vertical flow
WWTP	Wastewater treatment plant

Chapter 1

Introduction

1. Introduction

1.1 Context and motivation

1.2 Thesis objectives and outline

1.1 Context and motivation

In these modern times, available clean water is still no standard for everyone globally. Studies showed that in 2015 still 800 million people worldwide (11%) had no access to safe drinking water services nearby. On top of that almost 2 billion people also use water sources contaminated with faeces (IWA, 2016; WHO, 2018). Contrary to this shortage, first-world countries often use potable water to shower, wash the car or even flush the toilet. These expensive and unsustainable ways of living should be discouraged. To approach a solution for both problems, as much wastewater as possible should be treated and reused. Among the numerous known methods, constructed wetlands are gaining more confidence since the last decades.

A constructed wetland could be described as a certain area of land filled with media (gravel, soil...) and vegetation where wastewater is pumped through. Inside this system microorganisms will accumulate as a biofilm on the media and organic matter will be degraded. This natural way of purifying water is considered as a sustainable and low-cost alternative to the classic wastewater treatment plant (WWTP) (Kadlec and Wallace, 2009).

In order to improve wastewater treatment systems, as constructed wetlands, different numerical models are created. These models are used as a convenient tool to get a better understanding of the working mechanisms inside constructed wetlands (CW). Since the introduction of the Activated Sludge Model 1 (ASM1) in 1987 (Henze et al., 2000), various new models were introduced as further development of knowledge about the wetlands' internal processes. In order to achieve these improvements, accurate data is essential. Therefore this research aims at providing data for constructed wetlands modelling, based on the more recent Simultaneous Storage and Growth (SSAG) model (Hoque et al., 2008) and Constructed Wetland Model no. 1 (CWM1) (Langergraber et al., 2009). As a result the main goal would be the continuous optimization of the current CW technology, so clean water provided using ecological treatment systems could be implemented on a bigger scale.

1.2 Thesis objectives and outline

In researches of PISOEIRO *et al.* (2017); HO (2018) and PIZALIS (2018) respirometry was used to study different stoichiometric parameters from lab-scale wetlands. These simulated CW consisted of containers filled with gravel media for biofilm to grow on and were intermittently fed with different mass loads. As an extension in this research area, the objective of this thesis will be to use respirometry techniques from previous works to study full-scale operating horizontal subsurface flow constructed wetlands.

Investigating full-scale CW will result in new points of view, but will bring new challenges as well. Not only a method to obtain the samples has to be created, also the respirometry tests based on the research of Ho (2018) need to be adjusted, as a soil medium is tested instead of the gravel from the lab-size CW. Once the tests are running, the main goal is to collect 9 different soil samples from the operating CW (at 3x3 intersections). From these samples stoichiometric parameters as the growth yield direct on substrate (Y_H) and storage growth yield (Y_{STO}) can be determined. With this data differences in growth yields along the bed could give a better insight in the efficiency of the wetland and will be useful in the further development of parameter model designs based on CWM1 and SSAG model. Additionally, results could be compared with the studies using lab-scale wetlands to analyse the essential differences.

The thesis is divided in 5 different chapters. Starting with a short introduction in chapter 1, the state-of the-art in chapter 2 will provide the theoretical background of recent information involving different aspects of respirometry. This includes a brief description of constructed wetlands, a description of the used technique with the recent knowledge about it and at last, more information about the modelling parameters of interest in this research. Chapter 3 will clarify the specific methods and procedures performed during the tests, followed by chapter 4, which summarizes the obtained results and the corresponding discussions. To end, different interpretations of the measurements and calculations, as well as possible explanations for the results will be summarized to complete the thesis with a final conclusion and potential future research possibilities.

Chapter 2

State-of-the-art

2.State-of-the-art

2.1 Constructed wetlands

2.2 Respirometry

2.3 Calculations for the stoichiometric parameters

2.1 Constructed wetlands

2.1.1 Overview

To describe constructed wetlands various definitions could be considered. Nevertheless it can be defined as a natural part of land or transition area which is not completely flooded, nor dry. Additionally, the extant 'wetness' should be sufficiently present to provide an ecosystem to exist continuously. The water in a wetland can be fresh, salty, brackish, static or flowing. Wetlands can also be named as *swamps*, *marches* or *bogs* (Kadlec and Wallace, 2009).

Constructed wetlands are the by men produced (or 'constructed') imitations of natural wetlands. This is done with the main intention of using wetlands in wastewater treatment. Other intentions might be to control floods and to create various habitats. This sustainable method for wastewater treatment is based on an easy mechanism and is not expensive to provide, but a lot of space is needed. However constructed wetlands as WWTP are getting more noticed since the last decade. This results in an increased usage and research in this study area (Rousseau, 2017).

Different types of constructed wetlands for wastewater treatment can be distinguished. Mostly a classification is used based on the water flow through the wetland: free water surface (FWS), horizontal subsurface flow (HSSF), vertical flow (VF) or combined flow wetlands. The vegetation at every wetland could be present as floating plants, submerged or emergent plants. In this system the water will be cleared of larger parts of its present solids by natural filtration and precipitation, but also organic matter and small-scale removal of nitrogen, minerals or (heavy) metals could occur under certain conditions (Kadlec and Wallace, 2009).

Within wetlands, the vegetation is an essential part of the system because of several reasons. Firstly microorganisms (MO) are able to attach to the roots of the plants which facilitates biofilm growth. So this provision of active sites increases microbiological activity. Additionally small amounts of oxygen are released by plants, nutrients are absorbed and the growing roots in the ground would help to spread the flow and develop better hydraulic pathways. With these main advantages the commonly used types of macrophytes are *Phragmites australis* (reed), *Typha spp.* (cattails), *Scirpus spp.* (Bulrushes), *Nymphaea spp.* and *Nuphar spp.* (Waterlilies). Specific species are mostly chosen depending on the type of wetland and its climate around it (Brix, 2003; Dotro et al., 2017).

Constructed wetlands are suitable to use in different stages of a wastewater treatment process. Generally the wetlands are deployed as secondary treatment. Larger pieces are filtered and separated first using systems as septic tanks. This will reduce the amount of suspended solids by sedimentation. Subsequently, the reduction of present organic matter, nitrogen and remaining solids is achieved as a secondary treatment step (Kadlec and Wallace, 2009).

2.1.2 Horizontal subsurface flow wetlands

In the interests of this research, the focus will be put on horizontal subsurface flow wetlands (HSSF wetlands). As the name suggests, water flows in a horizontal way through the media from one side to another, with the water level below the surface. Due to the water-saturated media, lack of aeration and light, most biological processes inside HSSF beds are anoxic and anaerobic. Figure 1 shows the structure of a classic HSSF wetland. This wetland consists of an inlet pipe at the top with a distribution system for the influent, typically an distribution pipe or distribution layer. Subsequently the water flows near the roots of the vegetation through the used media. The treated water leaves the system at the bottom-end of the wetland. The water level is often held a couple of centimetres below the surface of the media so the top part is not flooded and the possibility to get a free water surface flow is excluded. HSSF wetlands are mostly used as secondary treatment for domestic wastewater (Dotro et al., 2017).

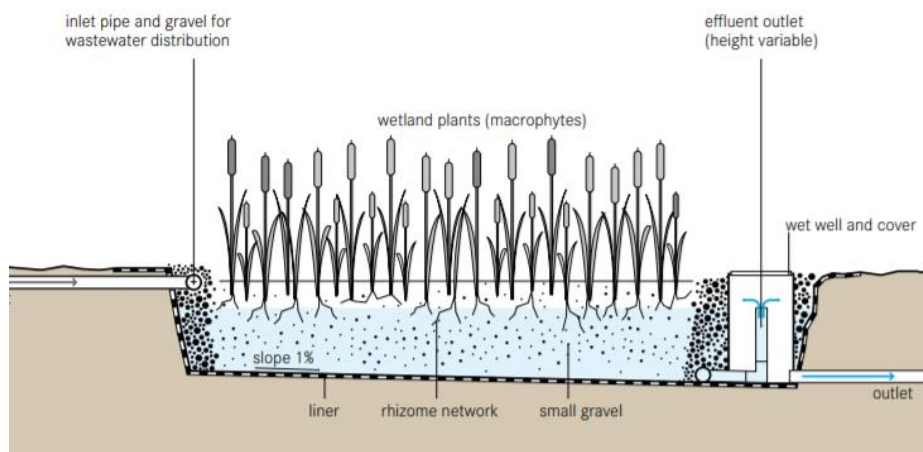


Figure 1: Typical HSSF wetland (Tilley et al., 2014)

The chosen type of media in wetlands can differ depending on the application. The importance of a right choice of used media is significant. Frequently used types are sand, gravel, stones or soil. Wetlands are generally designed with one type of media but occur as well with combined, layered media or in a mix. Decisions for a specific design depend mainly on the costs to provide it and on the particle size. The larger the size, the higher the possible water flow and different HRT, but smaller parts of suspended solids will be filtered worse. Moreover the possibility for substrate to adsorb at the media surface is usually inversely correlated with media size whereas larger media has the advantage to clog less too. For more consistent and accurate results, the used product should be clean, blunt and as equal in size as possible (Dotro et al., 2017).

The most common macrophyte species used in HSSF wetlands is *Phragmites australis*. This typical vegetation looks like a green plant with a $\pm 1 - 3$ meter high upright stem and small leaves of maximum 3 centimetres width. This species is known for its very invasive character, which makes it easy to provide at a wetland. Nevertheless the management of vegetation should be followed up carefully as an excess can influence the wetland efficiency and can cause a reduction of biodiversity. Common reed is also widely used for its excellent characteristics compared to other plant species such as higher photosynthesis rates, nitrogen- and carbon uptake. The roots nestle itself in the soil so well, it helps controlling the water level and acts like a natural flooding controller. Other functions of the plant are the uptake of metals and minerals (Brix, 2003; Chambers et al., 1999; Harrison, 2016).

Furthermore a small aerobic zone is supposedly present just near the roots and rhizomes of the plant. Atmospheric oxygen is inserted into the system via the stems and leaves to the roots. A part of the anaerobic conditions in fully water-saturated HSSF wetlands occur if the pores of the rhizomes are completely filled with water. This reduces the amount of oxygen and the low diffusion and solubility of oxygen in water will make the circumstances inside the bed often anoxic or anaerobic (Brix, 2003). According to Decamp (1996) the roots of macrophytes also help to create different hydraulic pathways. These two characteristics are summarized in the Root-Zone Method (RZM), or also called Kickuth-type wetlands. Other described characteristics include aerobic composting at the surface of the wetland area and microbiological wastewater treatment for HSSF-CW containing soil-clay media (Decamp, 1996).

Nevertheless according to Vymazal (2005) macrophyte HSSF beds with soil media are more likely to encounter difficulties caused by low hydraulic conductivities, regardless the implanted roots of *Phragmites australis*. These types of wetlands are a viable option for wastewater treatment at small loading rates and a low degree of pollution.

By stating that anoxic / anaerobic processes are of more importance in HSSF wetlands, the use of respirometry might be controversial. But despite the lower presence, (facultative) aerobic MO still significantly contribute to the wetlands' ecosystem and are considered in modelling studies. In addition, the use of respirometry in this application was successfully completed in works of Ho (2018); Pitzalis (2018), etc.

2.1.3 Clogging

Clogging is a term used in constructed wetlands when water flowing through the system is being obstructed. This could be caused by the presence of large solids, small media pore size, high water flow rate, etc. Consequences of clogging are higher flood risks and a reduction of contact time of the water with the biomass. When this occurs the system should be washed by reversing the water stream or the media should be removed. Pre-treatment steps are used to prevent CW from clogging. Different techniques are applied depending on the quality of the influent, wetland characteristics, price, required space and implementation / maintenance (Dotro et al., 2017):

- Solids and organic matter: larger molecules organic matter, (insoluble) solids and flocculated suspended solids are mostly removed using a settlement tank or septic tank which will separate larger pieces from the influent. If necessary further filtration steps could be implemented as pre-treatment. Smaller molecules BOD and COD (respectively biochemical- and chemical oxygen demand) dissolved in the influent will be oxidized by the MO inside the CW.
- Nitrogenous or phosphorous compounds do not significantly assist to the clogging of the system. Most of the molecules are dissolved and nitrogenous compounds are removed by nitrification. Only when a conversion into insoluble molecules happens, precipitation could take place. Therefore a filtration could be required.
- Pathogens can be removed by oxidation + adsorption, bacterial activity (at the roots), filtration or sedimentation. Natural removal is partially achieved inside the wetland.

Besides the pre-treatment steps, innovative and smart choices during designing and operating the wetland could decrease clogging possibilities (Dotro et al., 2017; Rousseau, 2017):

- During the design, increasing the wetland-width instead of the wetland-length could lower the '*cross-sectional organic loading rate*'. Thus clogging possibilities will be reduced.
- Selection of the right type of media and a proper loading rate of the influent.

- Prevention of an uneven distribution using a distribution system (e.g., distribution pipes). This decreases concentrated zones with a higher loading rate.
- Unwashed media with dirt or old rests of biofilm could stimulate clogging and should thus be avoided.
- Monitoring of the water level. Rising water levels could indicate clogging.

2.1.4 Modelling tools for biodegradation

To assist research, simulations of new ideas and potential developments are often executed first. These simulations are based on models describing different systems in terms of the present MO, processes or parameter calculation. This helps to create a primary result to verify how used systems would react to new changes (Brdjanovic et al., 2015). For wastewater treatment, purification and activated sludge systems, the activated sludge models (ASM) are ubiquitous. These models were created in 1987 by the International Association on Water Pollution Research and Control (IAWPRC). The increasing interests of research with activated sludge processes and the need for simple, easy-to-use models led to the design of new tools.

The activated sludge processes comprise the biological wastewater treatment process of sewage and other industrial / domestic wastewater (Scholz, 2016). Within this area, the expansion for good models especially on nitrogen-removal for activated sludge were coveted. Meanwhile the first model (ASM1), first published a few decades ago, was later enlarged with a second and third version (ASM2, ASM2d and ASM3) which include descriptions about the main water purification techniques such as phosphate / nitrogen removal (e.g. (de)nitrification) and COD / BOD reduction.

With the development of new models, more detailed processes and parameters are described to obtain a model matching reality as good as possible. During these expansions black box models are more and more being replaced by 'white box models'. But, by any means this global modelling language made research in this area easier and more efficient (Brdjanovic et al., 2015; Henze et al., 2000).

In the interests of this research, the stoichiometric parameters for respirometry procedures according to the **ASM1**, **ASM3**, **SSAG** model and **CWM1** are further investigated. Activated sludge models 2 and 2d will not be described because of the irrelevant content (P-removal) towards this research. (Henze et al., 2000).

ASM1 was one of the first models for the prediction of (de)nitrification and carbon oxidation in activated sludge processes. It was settled with 14 biokinetic parameters for 8 processes. Soluble units are named starting with 'S', particulate units with 'X'. Parameters are calculated based on different components, i.e., COD- and nitrogen components (figure 2). Within the COD-components a distinction is made between biomass (autotrophs or heterotrophs), non-biodegradable COD and biodegradable COD (readily or slowly biodegradable). Nitrogen-components include nitrates/nitrites and the total Kjeldahl nitrogen (TKN). This TKN is divided in ammonia, nitrogen from biomass and organic nitrogen (soluble / particulate and biodegradable / non-biodegradable) (Jeppsson, 1996).

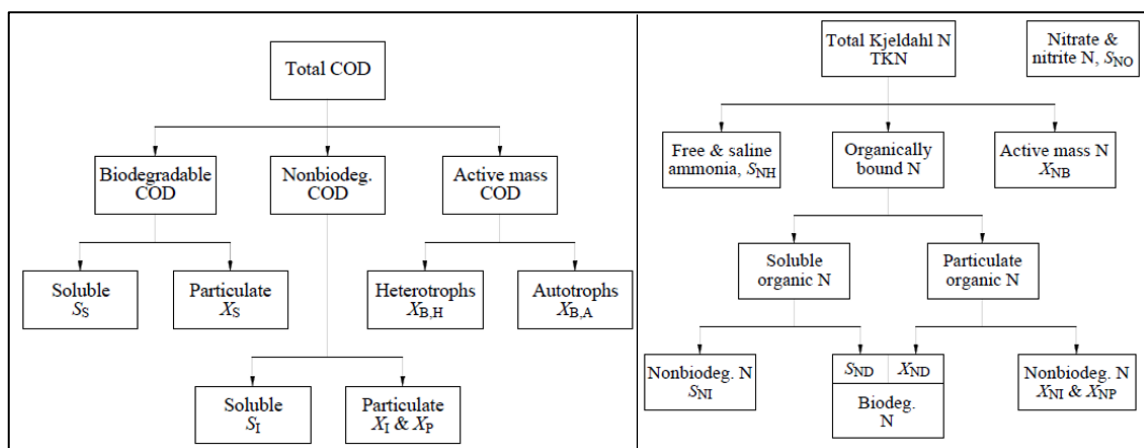


Figure 2: ASM1 subdivision of components (Jeppsson, 1996)

Nowadays, in terms of (aerobic) biodegradation of substrate ASM1 is considered insufficient to describe the processes. This model stated that the degradation of substrate using oxygen is only followed by direct biomass growth in a one-step pathway, without any consideration of the storage mechanism (Hoque et al., 2008).

Compared to ASM1, **ASM3** was designed with a different view on nitrogen and phosphorus removal, but most importantly the concept of storage was introduced for the first time. This storage phenomenon can be declared by a two-step biodegradation mechanism: an initial feast period followed by the famine period. During "feast-conditions", i.e. an excess in substrate, the MO use the energy from the substrate oxidation for cell maintenance and to form storage products. These storage products often consists of lipids or polysaccharides. Once all the substrate is oxidized and famine conditions occur, the storage polymers are used for cell growth and cell maintenance during the following period. Via this mechanism the MO accomplish their natural reaction to sustain during famine conditions. After the usage of all storage products, the system goes back to endogenous respiration (Henze et al., 2000).

Mathematically, most parameters from ASM1 and 3 are similar. The biggest changes are noticeable in the extra storage parameter, some little changes in the nitrogen compounds, different hydrolysis description and the change of decay processes to endogenous respiration. The 13 ASM3 biokinetic parameters and 9 processes are summed up in table 1 and table 2 (Henze et al., 2000). More details about stoichiometric and kinetic parameters will be discussed in “2.3 Calculations for the stoichiometric parameter”.

Table 1: ASM3 parameters (Henze et al., 2000)

Parameters	Unit	Parameters	Unit
S_O : Dissolved oxygen concentration	$M(O_2) / L^{-3}$	X_I : Inert particulate organic matter	$M(COD) / L^{-3}$
S_I : Inert soluble organic material	$M(COD) / L^{-3}$	X_S : Slowly biodegradable substrate	$M(COD) / L^{-3}$
S_S : Readily biodegradable substrates (COD)	$M(COD) / L^{-3}$	X_H : Heterotrophic biomass	$M(COD) / L^{-3}$
S_{NH4} : NH_4^{+} - and NH_3 -nitrogen	$M(N) / L^{-3}$	X_{STO} : Internal storage products of heterotrophic organisms	$M(COD) / L^{-3}$
S_{N2} : Dinitrogen	$M(N) / L^{-3}$	X_A : Nitrifying organisms	$M(COD) / L^{-3}$
S_{NOX} : NO_3^{-} - and NO_2^{-} -nitrogen concentration	$M(N) / L^{-3}$	X_{SS} : Suspended solids	$M(SS) / L^{-3}$
S_{ALK} : Alkalinity of the wastewater	$M(HCO_3) / L^{-3}$		

Table 2: ASM3 processes (Henze et al., 2000)

Processes*
Hydrolysis
(transformations to make slowly biodegradable substrates into more readily available substrates)
Aerobic formation of storage products from readily biodegradable substrate
Anoxic formation of storage products from readily biodegradable substrate
Aerobic growth of heterotrophs on storage compounds
Anoxic growth of heterotrophs on storage compounds
Aerobic endogenous respiration
(all forms of biomass loss / decay and cell growth at constant rates...)
Anoxic endogenous respiration
biomass loss / decay and cell growth at constant rates, but typically slower and based on nitrogenous compounds-usage
Aerobic respiration of storage products
Anoxic respiration of storage products
Aerobic growth of autotrophs
(due to nitrification instead of denitrification with heterotrophs)
Aerobic endogenous respiration of autotrophs
Anoxic endogenous respiration of autotrophs

**With all aerobic processes with heterotrophs using carbonous compounds to oxidize, and anoxic processes with heterotrophs using nitrogenous compounds do degrade.*

Despite the good fit from the model with experimental data, the main disadvantage of ASM3 appears to be an overestimation of the storage production. Therefore a modification of the ASM3 was designed. The Simultaneous Storage And Growth (**SSAG**) model. This model is similar to ASM3 but alternatively to the two-step mechanism, the SSAG model claims that during the feast period direct biomass growth from substrate oxidation as well as the storage phenomenon occur simultaneously. Only at a complete substrate depletion, the famine period will start and cell growth on only stored polymers takes place (Ortigara et al., 2011). During the research of Hoque et al. (2008) results for aerobic biodegradation of acetate according to the SSAG model resulted in the best fit with the data and could provide a realistic and achievable explanation for the processes. (Sin et al., 2005).

The last model, the **CWM1** is a resume of all important processes to predict the water effluent concentrations for VF and HF wetlands in aerobic, anaerobic or anoxic conditions (17 processes, 8 soluble – and 8 particulate components) without the prediction possibility for gaseous emissions. In contrast to ASM3, in CWM1 no description is incorporated about the storage mechanism. Although this comprehensive model is one of the most modern and accurate scripts, the use of it in respirometry would be more difficult because of the absence of the storage phenomenon (Langergraber et al., 2009).

2.2 Respirometry

2.2.1 Principles

Respirometry is a term used to describe the measurement of oxygen consumption. These biochemical processes, also called respiration, take place in the cells of heterotrophs and include the metabolic processes for the generation of ATP (adenosine triphosphate). This mechanism is presented in the following diagram:

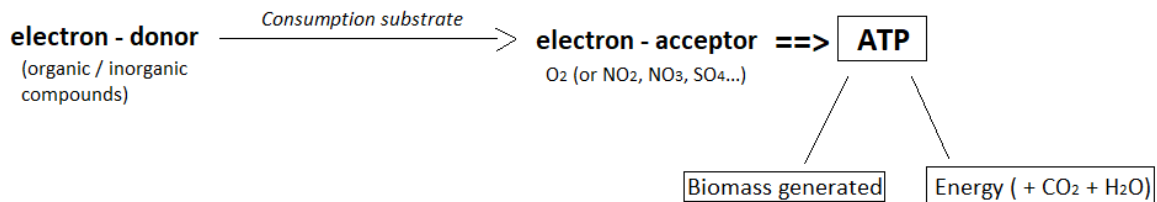


Figure 3: Cell respiration

During this respiration bacteria and other heterotrophic MO will oxidize different compounds to CO₂, water and energy. A part of this energy is used to maintain vital processes inside the cell, another part is used for the anabolic processes to generate biomass or to replace cells after decay (Vanrolleghem, 2002).

Spanjers et al. (2016) explained that by controlling the exact conditions inside a reactor (i.e. from the respirometer), the precise amount of oxygen consumption can be determined. Important is to control all the oxygen consuming processes, not only substrate-oxidation. Nitrification is often one of the main interferences during respirometry tests. During respirometry the concentration of dissolved oxygen (DO) is the primary parameter. The OUR or "Oxygen Uptake Rate" represents the speed of oxygen consumption, which indicates the different phases of the cell respiration. The total amount of oxygen consumed in the process can be plotted as a graph using the OUR-value. The different phases identifiable in the plot are explained in more detail later.

The most interesting parameters, but difficult to measure, would be the rate of substrate oxidation and biomass generating rate. However to obtain this information, parameters which are more easy to measure are used such as the oxygen saturation, oxygen transfer coefficient or amount of dissolved oxygen. From these results, values for more complex processes are calculated (Vanrolleghem, 2002).

Due to the relatively new concept of investigating the respiration during biological wastewater treatment, a lot of different ways of performing respirometry are available. During this research, methods following previous work of Ho (2018) are maintained, namely the use of an attached biomass respirometer, to allow for the test of gravel samples.

2.2.2 Respirometer

In order to perform a working respirometry-test, typical reactors are used. These reactors, are designed to measure the oxygen consumption during a specific period of time. This is also called the respiration rate (Vanrolleghem, 2002).

Respirometers mainly consist of an airtight box (reactor) partly filled with water or sample and the other part with air. Besides the box, several extra components and connections could be part of the respirometer. Different types of respirometers can be classified according to the phase where oxygen is measured, the gas phase or liquid phase. Subsequently, the respirometers are also classified according to the type of flow. Is the gas phase static or flowing? Is the liquid phase static or flowing? To name the different types of respirometers an abbreviation of three letters is used. The first letter names the phase where the measuring takes place, the second one stands for the flow in the gas phase, the last one is for the liquid phase, e.g., an LSF-respirometer: Liquid phase, Static gas, Flowing liquid (Galvão, 2017; Vanrolleghem, 2002).

A mass balance can be composed for liquid phase-measuring respirometers determining the dissolved oxygen (DO) concentration (assuming fully mixed conditions between the gas/liquid phase). This general equation can differ depending on the specific type of meter (Vanrolleghem, 2002):

$$V_L * \frac{dS_O}{dt} = Q_{in} * S_{O,in} - Q_{out} * S_{O,out} - r_O * V_L + V_L * K_L a * (S^*_O - S_O) \quad (1)$$

With:

S_O = DO concentration in the liquid phase (mg/l)

S^*_O = saturation DO concentration in the liquid phase (mg/l)

$S_{O,in/out}$ = DO conc. in the liquid phase entering and leaving the system (mg/l)

$K_L a$ = oxygen mass transfer coefficient (\pm aeration term) (h^{-1})

$Q_{in/out}$ = flow rate of the liquid entering or leaving the system ($\frac{l}{h}$)

r_O = respiration rate of the biomass in the liquid ($\frac{mg}{l.h}$)

V_L = volume of the liquid phase (l)

The used respirometer in this research is based on an LSF-type reactor. A visual image of the respirometer is shown in figure 4. DO concentrations of the water (liquid phase) before and after flowing through the respirometer is measured by DO-probes. Using LSF-respirometers aeration inside the reactor is prevented so no oxygen exchange between the gas- and liquid phase is induced (Gernaey et al., 2001).

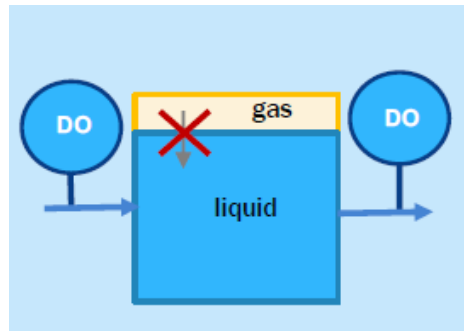


Figure 4: LSF-respirometer (Galvão, 2017)

Without this oxygen exchange between both phases, the K_La -value equals 0 and the mass balance (1) can be facilitated and written as in (2). For r_o , the value can be determined from S_o in and S_o out. But corrections must be made because of the measurement delay of those two values depending on the HRT (Vanrolleghem, 2002).

$$\frac{dS_o}{dt} = \frac{Q_{in} * S_{o,in}}{V_L} - \frac{Q_{out} * S_{o,out}}{V_L} - r_o \quad (2)$$

Important parameters during the measurement of DO-concentrations using respirometers are: the origin of the sample / biomass (the location of sampling, the local parameters during sampling, type of sample) and process parameters such as the type of substrate and how much is added, the HRT, volume water inside the reactor and weight and volume of the used sample, flowrate, temperature and which probes are used (Vanrolleghem, 2002). These aspects are discussed more in detail in “2.2.5 Process parameters” and during the description of the used methods.

2.2.3 Respirogram

2.2.3.1 Characterization of the respirogram

The measurements of the amount of oxygen during a certain time can be plotted in different graphs. The DO concentration plotted as a function of time is used during the measurement to obtain a first indication of the results or whether the system is in equilibrium, i.e. the MO in the sample have reached the level of endogenous respiration.

When results are processed the oxygen consumption is mostly plotted in terms of OUR (Oxygen Uptake Rate) which represents the rate of consumption of oxygen in $\text{mg O}_2 / \text{L} / \text{h}$. During this research the OUR is calculated by the difference of DO concentration from the inlet minus the outlet, divided by the HRT obtained after a tracer test (Andreottola et al., 2007). All the calculations and graphs of the respirograms are done automatically using a VBA-file in excel. This VBA-file is designed by Eng. Joana Piseiro. A further explanation about the calculations and used equations can be found in “2.3 Kinetic- and stoichiometric parameters”.

Normally, a typical respirogram, as shown in figure 5, can be divided in four important phases (Ortigara et al., 2011; Piseiro et al., 2017):

- 1) The initial endogenous respiration. A constant value of the OUR or DO concentration.
- 2) A fast rise of the OUR shortly after the substrate injection. This increase keeps going until all the substrate is used. When this happens the OUR will peak and will be followed by a fast decrease.
- 3) At a certain point the fast decrease stops and makes place for a slower decrease. This is the result of the depletion of substrate and the consumption of storage products.
- 4) Final endogenous respiration. All the substrate and storage products are oxidized and the OUR value / DO concentration is constant and stable. This level may be higher than the initial endogenous respiration level. According to the work of Piseiro *et al.* (2017), this could be the result of still ongoing processes / biomass growth or biomass and organic matter present in the measuring cell.

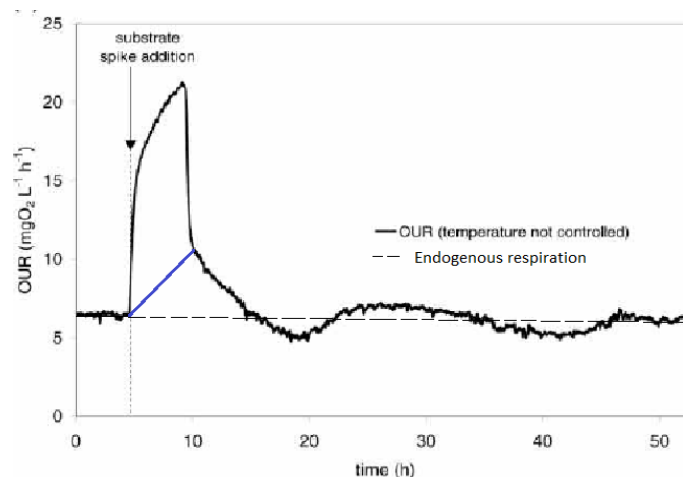


Figure 5: Respirogram (Ortigara et al., 2011)

Minor fluctuations will happen during tests (as shown on the respirogram). This common signal is mostly due to temperature fluctuations. To exclude the temperature influence and obtain a more stable result (especially at endogenous respiration level), the OUR profile is corrected with the temperature using the following equation¹ (Ortigara et al., 2011):

$$OUR_{corrected} = OUR * \alpha^{20-T} \quad (3)$$

With:

T = the actual temperature (°C) with 20 °C used as a reference temperature

α = correction factor (= 1.08)

Important to mention is that the previous described stages are common, but are not guaranteed to always be present. The production and use of storage products is assumed, but can in some circumstances be very low or absent. Furthermore different variations on OUR plots are studied during research of PISOEIRO *et al.* in 2017. The performed tests in this research resulted in three different kind of OUR profiles. Previous mentioned phases of a respirogram were somehow manifest in every type of profile, but varied. Figure 6 shows the different types.

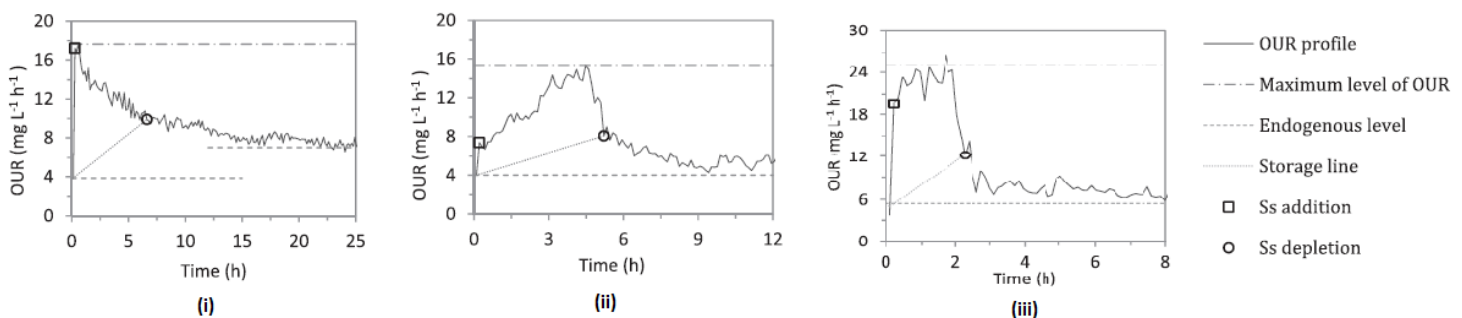


Figure 6: 3 different types of OUR profiles perceived in the study of PISOEIRO *et al.* (2017)

- i. The first and most common type starts with a fast and high rise of the OUR directly after the addition of substrate followed by a first decrease (still due to the consumption of the added substrate). When storage consumption starts a slower decrease is observed. This type is also known as a “fast starter”.
- ii. The second type of OUR profile, contrary to the first one, is a slow starter where only a very little initial peak arises right after substrate addition. Further, the OUR increases with a slower rate. When all the substrate is consumed, the value drops fast and storage is used at a lower rate similar to the first type.

¹ This calculation is automatically executed in the used VBA-file.

- iii. For the last type the OUR profile is characterized by a fast, high peak after substrate addition, followed by a constant OUR value that persists. This level represents the simultaneous substrate consumption and cell growth at a constant rate. After depletion of substrate the OUR drops fast and only storage products are consumed. This type is assumed to occur more with samples where the biomass is fed with higher organic loadings (Dizdaroglu-Risvanoglu et al., 2007).

Information about specific circumstances of the wetland could help to understand potential deviations in the results. According to the study of Galvão and Matos (2012) changes in organic loads on wetlands can influence the COD removal efficiency. So it can be stated that the microbiological activity in the biofilms of wetlands is adapted to the feeding pattern and specific environmental conditions.

No direct consensus is currently known on how wetlands should be treated to obtain only one specific type of OUR profile. A lot of parameters influence the system. Therefore factors as the quantity and quality of biomass are important. Also the HRT, feeding, temperature or pH should be taken into account (Pisoeiro et al., 2017).

To determine the total amount of O₂ used to oxidize the substrate the integral is calculated under the graph from the start of substrate addition to the top of the peak. Storage products can be calculated using the integral of the surface under the blue line on figure 5, excluding endogenous respiration. Differences in the respirometry tests compared to circumstances at the CW should be recalled. During the lab-tests, the water is fully aerated to determine the consumption from the excess in O₂. This is often a limiting factor in HSSF wetlands, therefore a small overestimation of certain parameters is presumed (Ortigara et al., 2011).

2.2.3.2 Endogenous respiration

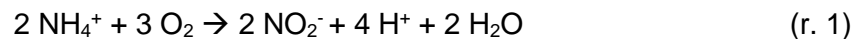
An important term during respirometry is endogenous respiration. In wastewater treatment a lot of processes are biologically driven. So the function and working mechanism of micro-organisms is very important. Endogenous respiration is used to indicate a level where bacteria, MO, etc. are using oxygen to maintain their vital processes. This oxygen is used in different aspects of metabolic processes inside the cells. But, the available energy obtained from oxidation processes is also used for cell growth. It is assumed that a higher rate of cell growth or -decay corresponds with an increased endogenous respiration. A different residence time or turbulence could disturb or influence the respiration rate, and the growth of biomass as consequence (Boone, 2016; Hao et al., 2010).

The water used at the inlet of the respirometry setup is oxygen-saturated. During the respirometry tests (especially at the level of endogenous respiration), it is advised to maintain a DO concentration higher than 2 mg O₂ / L to preserve a correct measurement. This 2 mg O₂ /L is a limit based on the work of Spanjers et al. (2016). Oxygen-limiting circumstances could occur when the signal drops below this level. Hypothetically considered, if these circumstances appear, anaerobic conditions exist in at least multiple parts of the reactor. This is avoided because of its disruption of the respirometric test. It usually indicates the consumption of oxygen by other organisms, interferences or other errors in the setup.

2.2.4 Interferences

2.2.4.1 Nitrification

One of the interferences likely to happen is nitrification. Nitrifying bacteria are frequently present in different WWTP (Andreottola et al., 2007). Nitrification starts with the oxidation of ammonium to nitrite (r. 1) by *nitroso bacteria* and is followed by the oxidation of nitrite to nitrate (r. 2) by *nitro bacteria*. This total reaction shows that 1 mole NH₄⁺ uses 2 mole O₂ and is followed by a decrease of the pH (Van Hulle, 2016).



When the nitrification process occurs during the respirometric tests, readily available BOD will be oxidized first. At the end of the oxidation, the nitrification process will start, followed by the further oxidation of slowly available BOD afterwards. Because of the oxygen consumption during nitrification and as consequence the big margin of error in measuring the OUR profiles for substrate oxidation, the use of an nitrification inhibitor could be, in that case, recommended (Van Hulle, 2016).

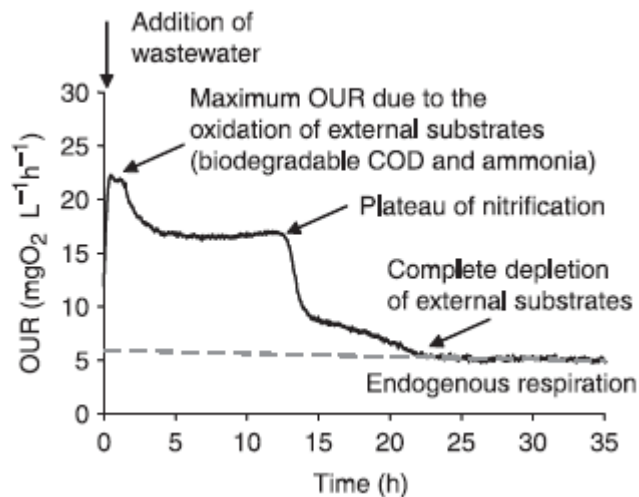


Figure 7: Respirogram with nitrification (Andreottola et al., 2007)

As previously stated, a classic respirogram contains a high peak of the OUR-value due to the oxidation of the substrate, followed by a fast decrease until it reaches endogenous respiration level again. When the nitrification process occurs during the tests, it would be observed at the measured respirogram. Andreottola *et al.* (2007) produced a typical OUR-profile with nitrification (figure 7). After an initial OUR-peak, the signal is followed by a constant signal which is better known as a plateau of nitrification.

If no nitrification takes place during the respirometry tests, no extra addition of inhibitors are necessary. If not, numerous inhibitors are available. A well-known and used inhibitor is NTH-600 ($C_4H_8N_2S$), or N-allylthiourea (Ortigara et al., 2011; Pisoeiro et al., 2017). These nitrification-inhibitors are often highly toxic for *Nitrosomonas* bacteria and depress the activity of the organisms. By reducing the cell metabolism, cell lysis is induced. It also has effect on the enzyme AMO (or ammonia monooxygenase), which acts as catalyst for the degradation reaction of ammonium (Interpro, 2018). The inhibitor will occupy the active sites of the enzyme so the activity decreases and it eventually gets inactivated (Zacherl and Amberger, 1990).

Other inhibitors frequently used are Nitrapyrin (or 2-chloro-6-(trichloromethyl)-pyridine), DCD (dicyandiamide) and DMPP (or 3,4-dimethylpyrazole phosphate). The working mechanisms of these inhibitors are very similar and are mostly based on the occupation of the active sites of the enzymes in the reactions to delay or even stop nitrification (Compo Expert Benelux nv, n.d.; Nave et al., 2017).

Denitrification could occur during anoxic circumstances. During the respirometric tests, this process is not considered as a possible interference. Anoxic state is avoided as much as possible, as the interests of this research lays in the aerobic oxidation of acetate. Following Van Hulle (2016) this last is thermodynamically more favourable.

2.2.4.2 Sulphur and iron bacteria

Oxygen consumption is mostly depending on two groups of components: Organic carbonaceous compounds and ammonium (+ other nitrogenous compounds). These groups are responsible for the biggest consumption of oxygen. Nevertheless another possible, but smaller, interference during respirometry is inorganic compound-oxidation. Especially sulphur and iron bacteria responsible for the oxidation of sulphide and divalent iron (Van Hulle, 2016; Van Loosdrecht et al., 2016).

The inorganic compounds (as electron donors) will be oxidized using oxygen as electron acceptor. *Sulphur bacteria*, e.g. are capable to oxidise H_2S or SO_3^{2-} to H_2SO_4 . *Iron bacteria* will oxidize Fe^{2+} to Fe^{3+} . During the process, CO_2 is used by the autotrophic bacteria responsible for these reactions and energy is gained. When this mechanism occurs, the biofilm attached to the media will get a bad odour, different colour, etc. and, in this research, respirometry tests could be influenced (Vanrolleghem, 2002). If no irregularities are detected, absence of sulphur or iron bacteria is likely as these bacteria are not always widely present in municipal wastewater. No further proceedings would be necessary in that case.

2.2.5 Process parameters

During the process certain important parameters need to be controlled or measured regularly. By changing different parameters the process can be influenced as demanded, but variations during the measurements could lead to insufficient data. Therefore a close and careful observation is necessary.

Temperature:

The temperature is one of the most important process parameters. Differences in temperature can affect the measurement on different levels.

- Reaction rates (of the aerobic respiration, oxidation of the substrate...) could be delayed or accelerated.
- Coefficients in the mass balance of the respirometer often depend on temperature or pressure (Vanrolleghem, 2002)
- The solubility of oxygen is temperature-dependant.

Because of these possible influences during the respirometric tests, the temperature is continuously measured. During the calculations the effect of the temperature on the results is consequently always taken into account.

Flow rate:

The flow rate is a required parameter to determine the OUR profiles. In order to verify a constant flow, the flow rate should be measured regularly. This parameter is also used in the mass balance of the LSF respirometer. Secondly, the flow is used as an adjustable parameter to obtain a desired HRT. In an optimal system the HRT is just high enough so the needed oxygen can be used for the microorganisms reactions, without using all the oxygen present in the water and an anaerobic state inside the system as consequence (Spanjers et al., 2016).

Volume:

The total amount of water in the system during the tests should be constant to maintain an accurate result. From this volume of water inside the reactor a first indication of the HRT can be calculated while a confirmation of this value is fulfilled with a tracer test afterwards.

Sample volume and weight:

The sample volume and weight are necessary values for further analyses after the respirometric tests to determine the total amount of biomass.

Ambient light:

When the system is set-up and the test is running, the reactor and measuring cell should always be covered as much as possible. Ambient light could cause disturbances particularly at the optical DO-sensor. This sensor is very light sensitive and should therefore be isolated from light fluctuations to maintain a stable signal. For the reactor, the light could interfere and stimulate photosynthesis by certain MO in the sample (Spanjers et al., 2016).

pH:

Measuring pH can help to indicate some ongoing reactions inside the biofilm. During the respiration- and oxidation reactions in the cells of MO pH changes could be detected. A constant interaction between proton production and consumption is present. When the concentration of protons suddenly changes drastically, this could be the result of unwanted reactions (e.g. CO₂ release, (de)nitrification, ammonium uptake...). If pH fluctuations are observed, adjustments as acid/base-additions or changes in the operating tests could help controlling the system. For a well-balanced system without nitrification or other unusual reactions, pH variations are exceptional (Gernaey et al., 2001).

F:M-ratio (food to microorganisms ratio):

A well balanced F:M-ratio is required so the reaction inside the reactor would cause a clear oxygen consumption peak, followed by a decrease and potential storage consumption. The exact concentration used is necessary during the calculations to determine the OUR-profiles.

2.3 Calculations for the stoichiometric parameters

Currently the SSAG model seems to be the most accurate model to describe respirometry tests (Ortigara et al. (2011); Piscoiro et al. (2017) and Sin et al. (2005)). Parameter estimation will therefore be based on this model. Figure 8 summarizes the process schematically as explained by Hoque et al. (2008).

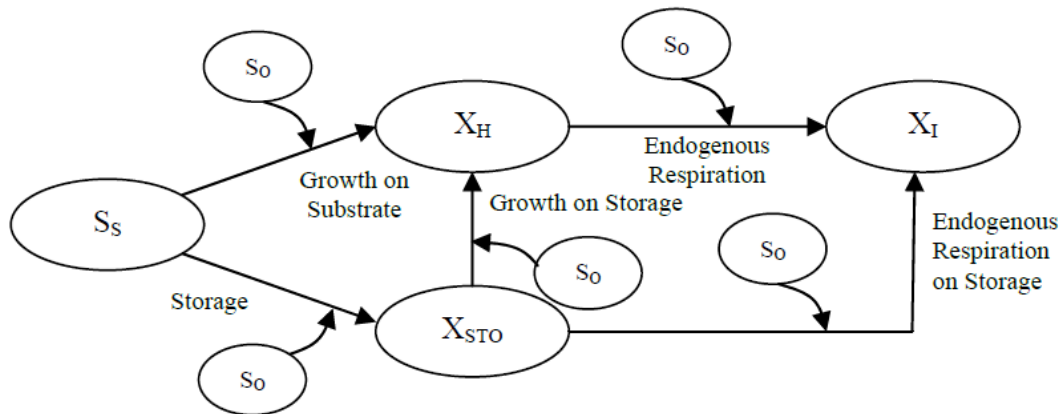


Figure 8: Schematic overview of the SSAG model (Hoque et al., 2008)

Although the theoretical model assumes the simultaneous storage and growth process to be indisputable, no information is currently available about the distribution between both processes. Because of the uncertainty of a possible mathematical relationship, calculations are executed without any distinction between the biomass growth on substrate or on storage products. Nevertheless, storage growth is calculated following a linear relationship as shown in figure 9 (Piscoiro et al., 2017).

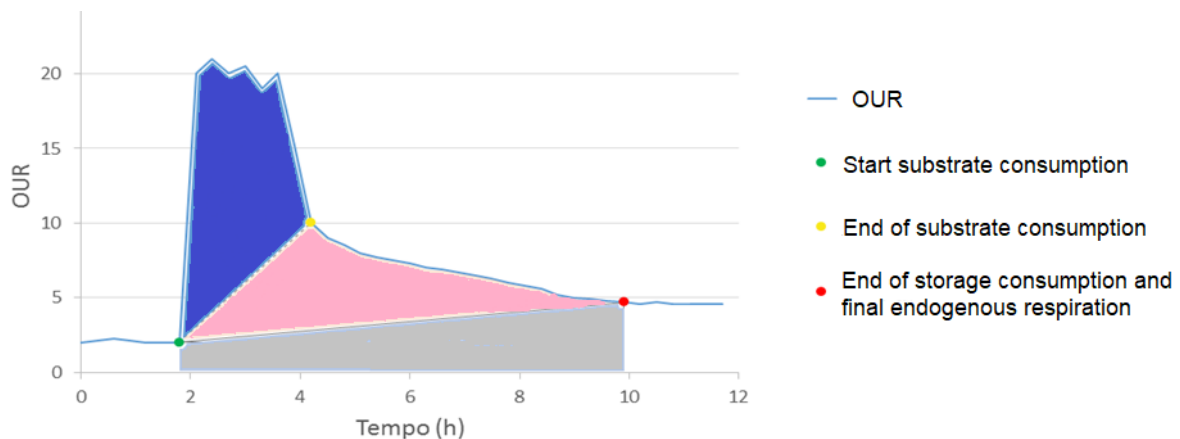


Figure 9: Calculations on the respirogram (Piscoiro, 2018)

The total integral of the measurement is calculated from the moment substrate is added (green point - start) until the point endogenous respiration level is reached again (red point - end), with the yellow point in the middle (= middle) at which all the substrate is consumed and only storage products are used. The grey surface represents the endogenous respiration during the tests. During calculations, the start, middle and ending of the tests are visually determined. The total surface of the OUR-curve can be divided in 3 main parts:

- The integral of **substrate consumption** (blue)
- The integral of **storage consumption** (pink)
- The integral of **endogenous respiration level** (grey)

From this the following yields are calculated:

$$Y_H = 1 - \frac{\int_{Start}^{Middle} \text{Substrate consumption}}{\text{Feeding}} \quad (4)$$

$$Y_{STO} = 1 - \frac{\int_{Start}^{End} \text{Storage consumption}}{\text{Feeding}} \quad (5)$$

With:

Y_H = initial growth yield on substrate (mg COD biomass/mg COD substrate)

Y_{STO} = storage yield (mg COD storage/ mg COD substrate)

$$\text{Feeding} = \frac{V_{\text{substrate}} (l) * C_{\text{substrate}} (\text{in COD-mg/l})}{V_{\text{water in reactor}} (l)}$$

A short summary of the main processes based on the SSAG model stoichiometric parameters is given in Appendix A. This matrix includes the calculated Y_H and Y_{STO} and includes an extra parameter $Y_{H,STO}$ (growth yield on storage products). The validation of this model with all three parameters is excluded within this research, due to the difficulty to distinguish both Y_{STO} and $Y_{H,STO}$ in an accurate way, as mentioned earlier.

Revision of the literature review and objectives

From this background knowledge different objectives of this thesis could be motivated. One of the most important motives for this research, is the further development of constructed wetland models. The vision of constructed wetlands as 'black-box' models do not include different growth patterns of microorganisms throughout the bed. Because of the lack of knowledge about these processes, investigation regarding possible different microbiological characteristics across a wetland bed could help to get a better understanding of the inside working mechanisms. In line with this objective more data is necessary about physicochemical and stoichiometric parameters in fully operating soil based wetlands. By providing more data, it could help to develop further modelling tools as the ASM3 or especially the SSAG model and CWM1.

It is of big importance to use a reliable method is in order to collect the necessary data stated above. The use of LSF respirometers for fixed biomass testing of HSSF CW showed promising results in earlier researches. Within the framework of this study, a further usage of this method was handled. This with the aim to adjust and improve the tests so a reliable standard method could be proposed.

A last important note is the choice of sodium acetate as used substrate. The main reason for this choice is the use of it in previous work regarding respirometry and / or constructed wetlands (Ho, 2018; Piseiro et al., 2017; Hoque et al., 2008). Besides, acetate solution is a simple and readily available organic compound to oxidize during the tests, which is recommended during the respirometric tests (i.e. no slow BOD). Also no nitrogen is added when using acetate. This will help to minimize possible problems regarding nitrification interferences. With these arguments in mind, optimal circumstances were planned to obtain respirograms only for the determination of Y_H and Y_{STO} .

Chapter 3

Materials and methods

3. Materials and methods

- 3.1 Investigated full-scale operating wetland: Barroca d'Alva
- 3.2 Sampling methodology
- 3.3 Respirometry test
- 3.4 Post-measuring

3.1 Investigated full-scale operating wetland: Barroca d'Alva

Barroca d'Alva is a small place in Alcochete (Setúbal district), located to the east of Lisbon across the Tagus river (figure 10). The constructed wetland at this location is an operating WWTP consisting of 4 different HSSF beds with a surface of 425 m² (20.8 x 20.3 m) and a depth of 1.05 m, each. Every bed is planted with *Phragmites australis*. Barroca d'Alva is designed for the treatment of wastewater originated from a short number of houses, a local tv-station studio and rural hotel. All together it would serve ± 500 inhabitants. Currently, due to tv-station not using the studio, only 100 inhabitants are served with a daily average water consumption of 150 L / inhabitant / day.

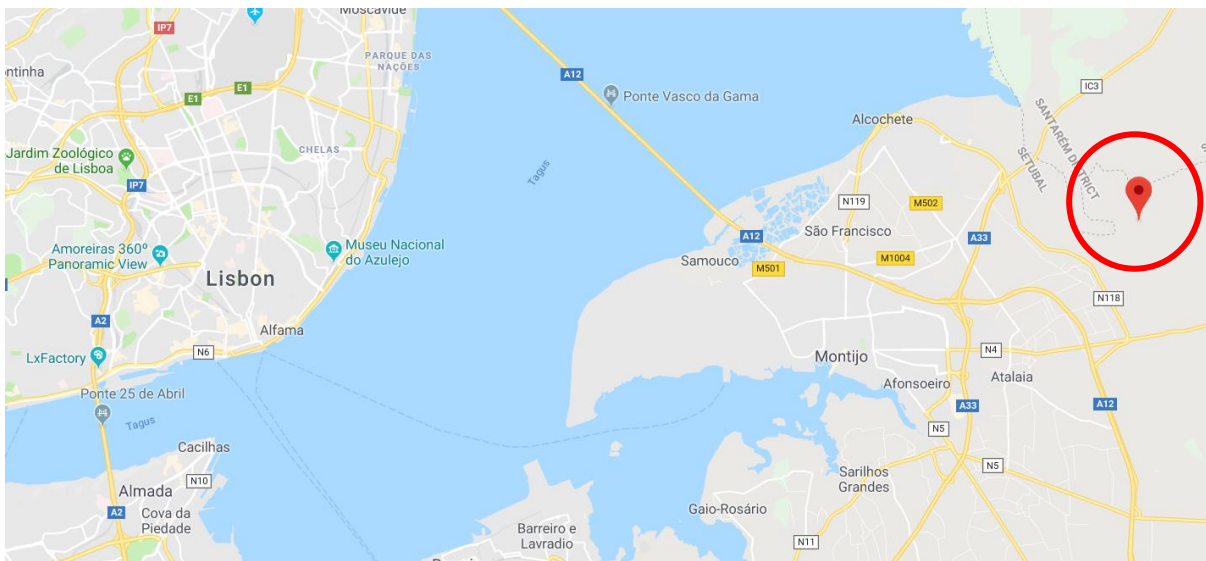


Figure 10: Location of the WWTP

During the purification the to be treated wastewater is subjected to a pretreatment step by entering a septic tank first. This has as function to separate bigger solids by sedimentation. Thereafter the water gets divided in four different streams, one for each of the existing wetland areas present at the WWTP.



Figure 11: Constructed wetlands Barroca D'Alva

To obtain get a better insight of the investigated wetland, manholes were opened at the in- and outlet of the wetland area. However, a high amount of mud/dirt was observed at the inlet together with a low water level, so no influent was entering the bed. At the outlet, no continuous flow of water discharge was leaving the wetland. This observation could be linked to the periodic pump cycles of the WWTP. Due to the small amount of wastewater to treat, the pump only works a few times a day. After pumping, the septic tank will discharge influent that will flow into the wetland. This goes on until equilibrium is reached again and the cycle gets to an end. As a result the wastewater flow will be low or null most time of the day.

Within the framework of this research, measurements of the water quality and wetland efficiency were excluded. In table 3 an overview is attached with the influent- and effluent concentrations of physicochemical- & microbiological parameters measured between 2006 and 2018. The values of different parameters show a rather constant trend, with a few exceptions. Nevertheless, most components were measured within the emission limit. The wastewater treatment plant is designed for average annual inflow amounts 60 m³/day and a peak flow up to 251 m³/day. Extra data of influent and effluent concentrations of the wetland obtained between 2002 – 2005 is provided in Appendix B: Results for the constructed wetland influent and effluent concentrations.

Table 3: Constructed wetland influent and effluent concentrations (2006 - 2018)

Physical and chemical parameters		24/10/2006		13/02/2008		11/05/2009		21/06/2018		Emission limit
		IN	OUT	IN	OUT	IN	OUT	IN	OUT	
pH	(-)	7.7	7.5	7.4	7.4	7.5	7	7.6	8.2	6.5-0-9.5
BOD ₅	(mg/L O ₂)	68	31	74	7.1	40	32	160	13	40
COD	(mg/L O ₂)	150	56	140	12	75	40	270	46	150
Total Phosphorus	(mg/L P)	4.6	2.1	4.3	2.7	2.9	2.1	5	8	10
Total Nitrogen	(mg/L N)	33	21	46	15	45	13	40	<5	15
Oils and Greases	(mg/L)	5.1	1.4	5.5	1.7	1.4	1.3	13	<5	15
TSS	(mg/L)	37	16	16	6.6	21	22	130	51	60
Microbiological parameters		24/10/2006		13/02/2008		11/05/2009		21/06/2018		
		IN	OUT	IN	OUT	IN	OUT	IN	OUT	
Total coliforms	(NMP/100ml)	16000	350	30000	500	160000	16000	2200000	2400	
Faecal coliforms	(NMP/100ml)	90000	170	1600	130	92000	16000	54000	920	
Streptococcus	(NMP/100ml)	16000	1600	5000	2	16000	9200	240000	120	
Helminth Eggs	(-)	-	-	-	-	-	-	Negative	Negative	
Salmonella	(Em 1000ml)	Negative	Negative	Negative	Negative	Positive	Positive	Negative	Negative	

3.2 Sampling methodology

The main goal is to obtain samples from different points in the wetland where certain parameters of that area will be determined. With these parameters the specific characteristics of this wetland could be mapped. This would help to get a better understanding about the internal processes inside constructed wetlands. In order to accomplish this, the investigated wetland area was divided in 3x3 intersections as represented in

figure 12 (distances and naming of the samples further used in the text are based on this representation). The water flow direction is marked by the blue arrow. One sample was taken for each intersection. One extra sample was collected (4A) to verify a developed hypothesis caused by unexpected difficulties at sample point 5.

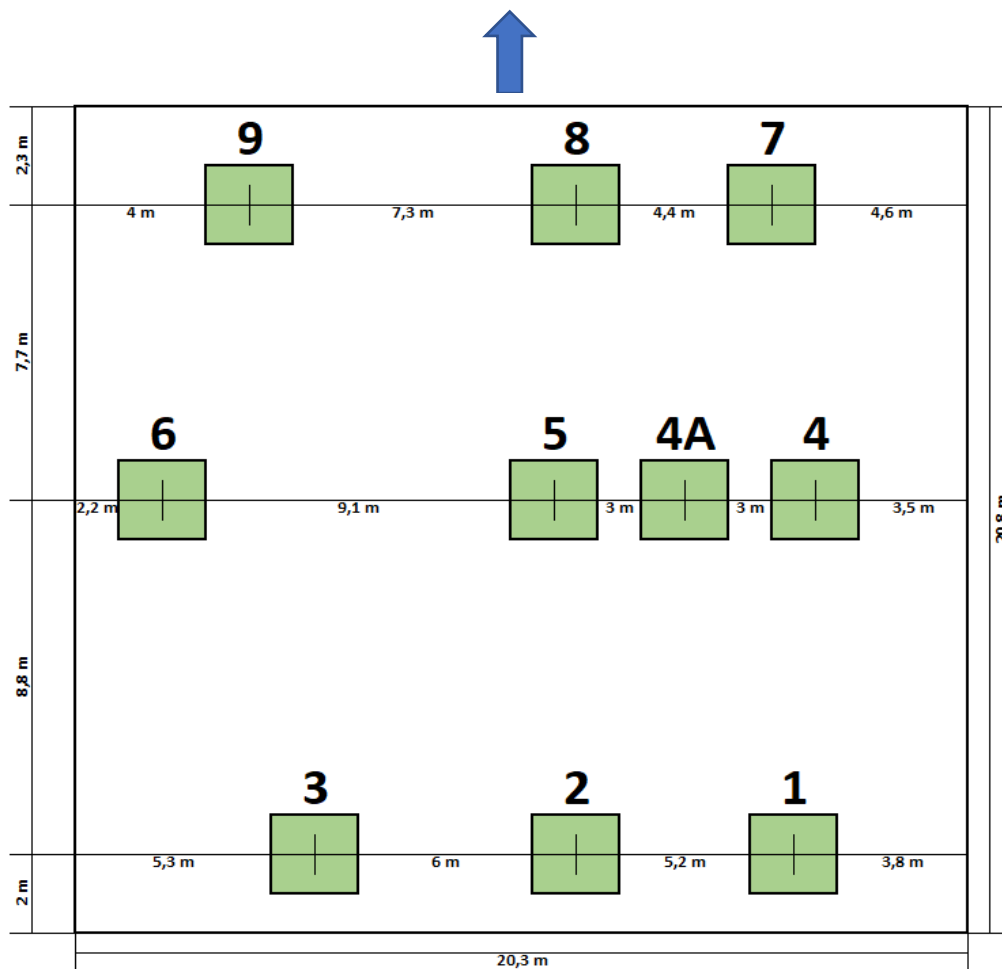


Figure 12: Map of samples taken, with distances.

Multiple sampling techniques were tested. At first the sample was taken by digging a little well into the soil and to extract the sample with a clamp (scissor – shovel shaped). Considering the compression of the sample when extracting with this tool, this method was rejected for further use. Benefits of this method was the ease to collect sample at bigger depths without much effort and the minimization of destroyed ecosystem.

As improvement of the first sampling method a different tool was developed. Figure 13 shows the 'extraction tube'. This 30 cm long plastic tube with a diameter of 19.2 cm, provided with notches at one side was partly inserted into the soil of the wetland. The use of a small shovel helped to break through obstructing roots so soil could be collected. By pushing the tube deeper, samples at different depths could be obtained without having the hole collapsing. With the aim of a good repeatability samples were collected from a depth of 15 - 20 cm. These samples were retrieved above the water surface. However, soil at this depth has a high moisture content. Maintaining this method resulted in an easy way of acquiring the desired samples without compressing it heavily, as it was gathered by hand. Moreover the emerged wells could be filled again with the upper layer of the wetland initially removed, so unnecessary disruption of the ecosystem was prevented.

Collected samples were preserved in airtight plastic buckets at room temperature without addition of water, until used for the tests (7 days approximately).



Figure 13: Sampling tube

3.3 Respirometry test

3.3.1 Setup

An illustrative representation of the laboratory setup is shown in figure 14 to describe the applied test mechanism based on studies of Ho (2018). This setup was assembled and used at the environmental lab at Instituto Superior Técnico (ULisboa).

In order to perform tests through respirometry techniques, the collected sample was placed in the reactor of the respirometer where oxygen-saturated water was directed in a horizontal flow through the sample. The DO-measurements at the inlet and outlet were obtained such that a total oxygen consumption inside the reactor could be calculated. Using a valve at the entrance of the reactor, an acetate solution was injected into the system to measure its behaviour during substrate oxidation.

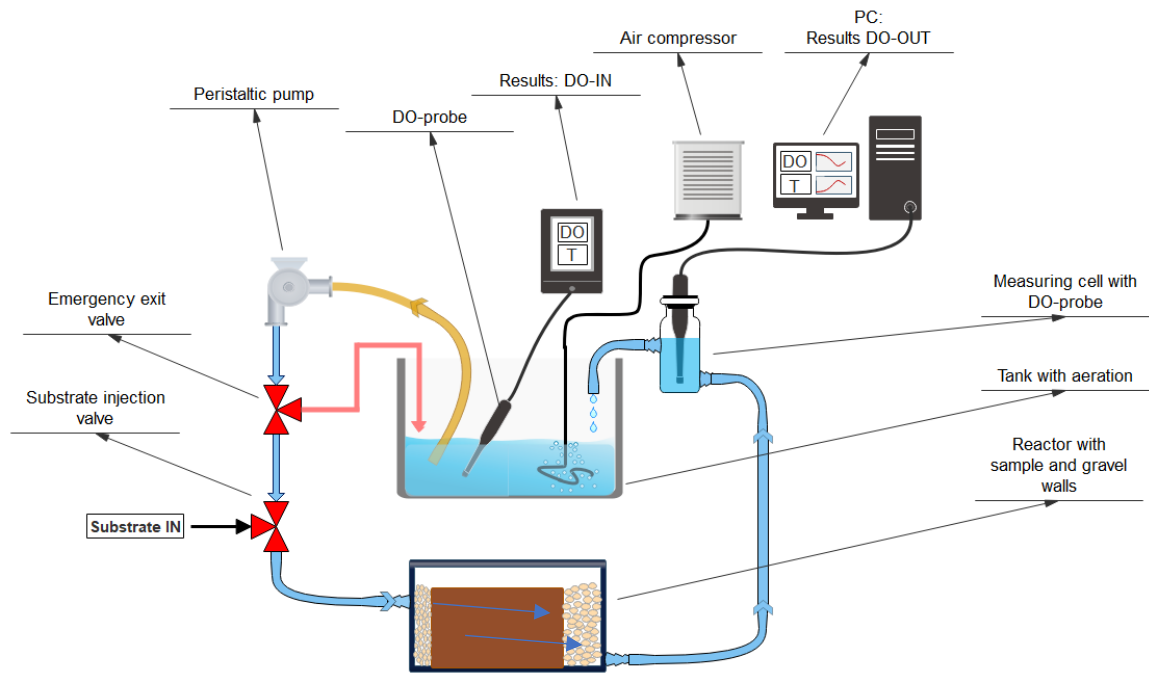


Figure 14: Representation of the LSF respirometer test setup

- An **air compressor** (AirMac DB-60) connected with a perforated flexible rubber tube was used to aerate the recirculating water to maintain oxygen saturation. From this constant value the difference in concentration was measured so the total consumed oxygen inside could be calculated.
- The DO-probe in **the tank** was used to measure the oxygen concentration and temperature of the water entering the reactor. Because of the stable value, less frequent readings were necessary. For this, the **multiparametric probe** (YSI 556 MPS - with electrochemical DO-sensor) was used with a measuring interval of 1 reading every 20 seconds.
- For water transportation with a constant flow a **peristaltic pump** was used (FWT VPER-N).
- As anticipation for potential problems or obstructions, an **emergency exit** was provided. The water would be directed by the 3-way (open) valve back into the tank so no flooding would happen.
- The **second valve** (3-way normally closed) was used to inject the acetate solution.
- After flowing through the reactor the DO-concentration and temperature were measured in the **measuring cell** with the **optical DO-probe** (YSI ProODO). This probe (with readings every second) was directly connected to the computer which plotted the real-time graph of the results during the tests. Afterwards, the water was guided back into the tank.

During the respirometry tests, two different probes were used to measure the necessary parameters such as the DO concentration and temperature. These were an optical probe and a multiparametric (membrane) probe. This luminescence-based electrode is one of the most important probes used because of its quick and sharp responses with stable measurements and the ability to measure these values properly even at low concentrations. The multiparametric probe is used for its lower price, less fragile components (contrary to the sensitive bottom of the luminescence DO-probe) and multiple functions in one probe (Windsor et al., 2012).

3.3.1.1 LSF respirometer: box reactor

A plastic box of 16 x 10.5 x 11 cm provided with an airtight lid was used as reactor in the LSF respirometer set up. Respirometry tests were initially performed with an identical respirometer used during the research of Ho (2018). However, an adjustment of the reactor was required due to the laborious water flow through soil samples and the dirt coming along. Several prototypes were evaluated: the addition of different filters, gravel at one side, gravel in a curved wall, gravel as little beam at the outlet. As a result, two straight gravel layers were introduced by taping meshes inside the box as support for the gravel (figure 15). At the inlet a small layer was inserted for better water distribution inside the reactor. The second one, large enough to decrease the overall pressure drop, improved the hydraulic conductivity and acted as a natural filter for dirt at the outlet.

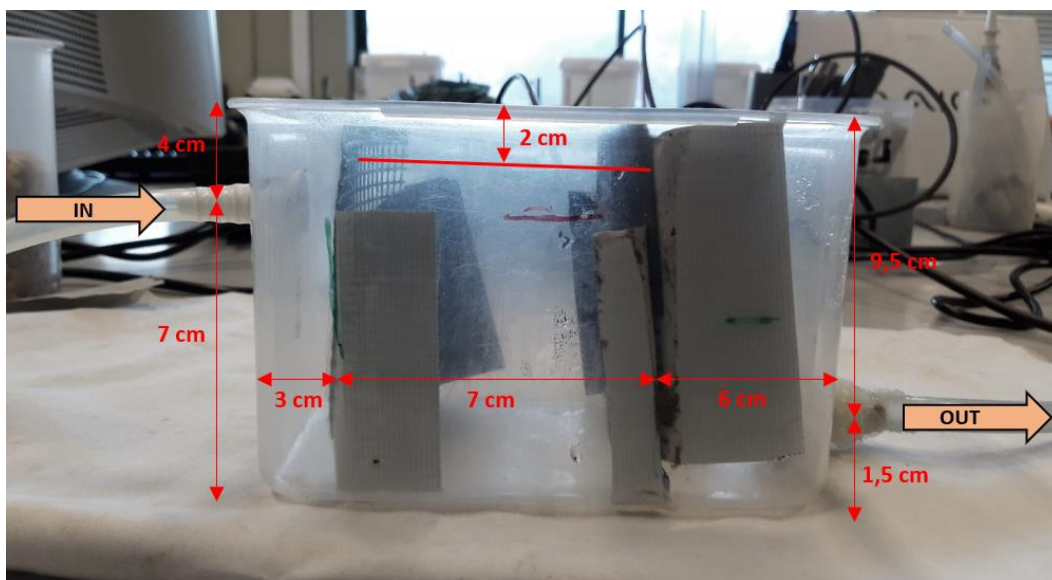


Figure 15: Adjusted box reactor of the LSF respirometer. Grey areas are the tape used to secure the mesh.

Figure 16 provides a better view inside the reactor. To ensure a better contact between the flowing water and all the biomass, the upper half of the second mesh was taped.

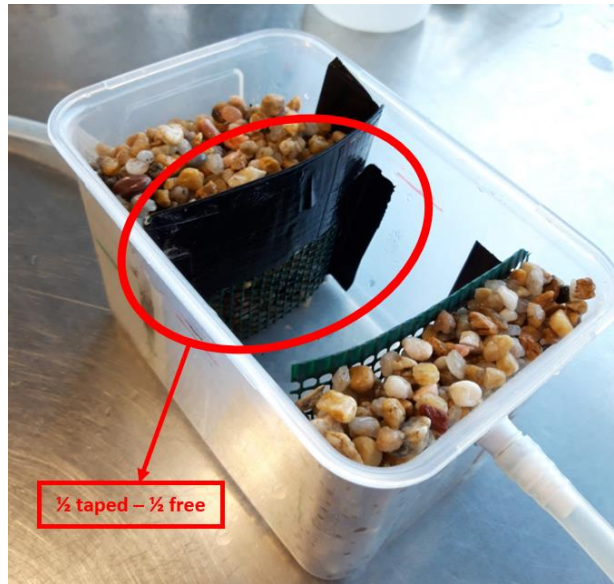


Figure 16: Inside view of the box of the LSF respirometer

When placing the sample, the box was filled for $\pm 80\%$ of the total height with sample leaving the remaining 20% with air (lid included). This corresponds to a volume of sample of approximately $500 - 600$ ml (figure 17).



Figure 17: Filled reactor of the LSF respirometer

3.3.2 Preparation

Initial cleaning:

Together with changing samples, all parts of the system were cleaned. This was achieved by an alternating wash with bleach, soap and enough water. With this disinfection, remaining MO were killed. An extra wash with plenty of water was done on the used gravel in the respirometer before introducing it back into the reactor. This to assure a complete elimination of attached biomass from tests with previous samples which could interfere.

Calibration:

In order to obtain a correct measurement, a calibration of both DO-probes was completed by measuring the oxygen concentration in the same cup. This calibration was repeated by the start of every new sample, occasionally also in between different tests from one sample if a deviation of the signal was suspected. With this step the remaining differences in time and oxygen concentration between both probes were acquired to correct the results during calculations. By measuring the deviation regularly, large differences were prevented. With the calibration included, corrections going from 0.2 mg O₂/L to 1 mg O₂ mg O₂/L (maximum) were used during the calculations.

Washing period:

When first running the system with fresh sample, a 'washing period' was sustained for ± 48 hours. During this time, the water would flow through the sample at a low flow rate (± 10 ml/min) so the excess of biomass and dirt would be washed out of the reactor. This is done with the assumption that most attached biomass would maintain inside the reactor, so no complete washing out of the biomass (BM) takes place. The water is in this case, not circulating but just discharged. Doing this, interferences of turbidity and dirt were minimized. In addition, this period is very important and necessary in order to reach an equilibrium where the MO are at endogenous respiration level. The duration of this 'washing period' was adjusted depending on the used sample. Only when both requirements were fulfilled (i.e., a constant DO signal at the outlet + no more dirt coming with the effluent), the tests could be started.

Volume measurement:

After executing the respirometry tests, different parts of the system as the tank and measuring cell were cleaned with water. Simultaneously the respirometer was drained, followed by the measurement of the total volume of water present in this part of the system during the tests.

Substrate preparation:

If required, a 0.05 mole/l sodium acetate solution was prepared based on the concentration used by Ho (2018) (1 g / 150 ml = ± 950 mg COD/ L). Determination of the exact COD-content of the used sodium acetate solutions was realised applying method 410.4 as described by O'Dell (1993) and using the 'spectroFlex 6600' spectrophotometer for analysis (λ = 600 nm).

Two different acetate solutions were used during the complete research. Firstly the acetate solution with a COD-content of 961.4 mg/L which was measured in the research of Ho (2018). After emptying this solution, a new solution was prepared and measured on 13th of November 2018. This was used until the 26th of January and had a concentration of 2908.7 mg/L.

In order to replicate a sodium acetate solution with a similar concentration, 1 g / 150 ml solution prepared (as indicated by the first acetate solution). However, a large difference in COD-concentration was measured. Plausible explanations include the miscommunication of used concentrations. Which led to acetate solutions with different molarities. Other possible influences may be induced by the use of a different sodium acetate stock (trihydrate or not hydrated). Mistakes executing the COD cuvette test could also influence the exact concentration. Degradation of the stock solution was measured multiple times and showed stable results.

3.3.3 Test procedure

For one sample, different tests were executed. Table 4 summarizes the necessary steps performed for one respirometry test. After these actions data would be available from the test. When the system settled back at the level of endogenous respiration, without renewing the soil, a new test could be executed repeating the steps described in table 4. Depending on the available time, approximately 3 to 4 tests were performed for every sample point (3-4 tests / 1 soil sample).

Table 4: Description of the operating procedure

No.	Action
1	Check-up if everything is connected properly.
2	The gravel and sample were positioned in the open reactor.
3	4 - 5 L tap water was added in the tank.
4	The pump was turned on, starting at a low speed.
5	When the water level inside the box almost reached the surface of the sample and the water is flowing from the measuring cell back into the tank, the reactor was closed with the air- and watertight lid.

-
- 6** The aeration of the system and the measurement by both probes were started. In the tank, the recirculating water should be aerated first before being measured and pumped.
-
- 7** After reaching an equilibrium and a constant flow (takes approximately **± 10 minutes**). The flow rate was determined by collecting the water draining from the measuring cell for 1 minute.
- $$Q = V / t \quad [\text{ml/min}]$$
-
- 8** The pumping speed was adjusted (if necessary) in order to obtain a flow rate of **15 – 20 ml/min**. After this adjustment the flow rate was measured again after reaching equilibrium. If the water level rises too much with increasing speed, a lower flow rate was maintained. Once the flow rate is acceptable and constant, the pumping speed is held unaltered.
-
- 9** The system was retained running uninterruptedly for at least **2 hours** or until the DO signal remains constant (at endogenous respiration). To prevent interferences from light, the system was covered as much as possible with a blackout fabric.
-
- 10** A new measurement of the water flow rate was executed.
-
- 11** After stopping the pump, **2 – 5 ml substrate** (sodium acetate solution) was injected into the system using a micropipette.
- The appropriate concentration should be estimated during different tests according to the used sample / system. The concentration should produce a DO-signal where a clear oxygen consumption peak is perceptible without dropping below 2 mg O₂ / l.
-
- 12** The measurement was maintained until the oxygen level settled back at endogenous respiration level and the test is finished.
-
- 13** A last measurement of the flow rate took place.
-
- 14** End of the test and extraction of the test data.
-

3.4 Post-measuring

3.4.1 Tracer test and hydraulic retention time

In order to obtain more information about the way the water flows through the reactor of the respirometer or how long it takes for the water to circulate in the system, the hydraulic retention time (HRT) was measured with changing sample. Calculations for the specific HRT of each sample were based on the “step-change integral modelling methodology” studied in the work of Bonner *et al.* (2017). The main principle of this technique is to keep adding a constant concentration to a system where the rising conductivity is measured until the maximum concentration of the applied salt-solution is reached. Applying this method, firstly conductivities of 0.0200 g NaCl additions in 200 ml tap-water were measured to produce a calibration line. For every test, a new calibration curve was composed. Before starting the test, the soil was fully saturated with tap water to maintain an equal repeatability (less different initial water contents between the different tests). With this data a 5 L salt-solution of 0.35 – 0.40 g/L (depending on the calibration) could be prepared. Using this solution as input the tests were started measuring the conductivity of the outgoing water stream. As effect, the result presented a conductivity – time graph with rising conductivity by different steps until the maximum was reached (figure 18). This maximum equals the concentration of the prepared solution (C_{max}). During the calculations, the area above the curve was calculated.

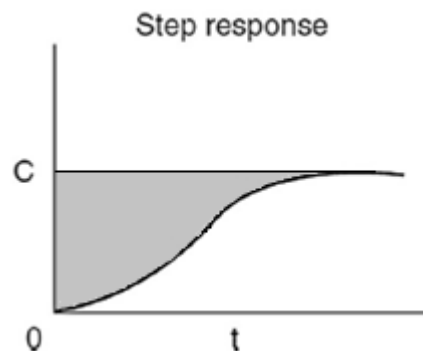


Figure 18: Tracer test step response graph (Bonner *et al.*, 2017)

From the performed calibration, the measured conductivity could be converted to a concentration. Further, the HRT could be calculated using equations (6), (7) and (8).

$$F(t) = \frac{C(t)}{C_{max}} \quad (6)$$

$$HRT = \int_0^{\infty} [1 - F(t)] dt \quad (7)$$

$$\sigma^2 = 2 \int_0^{\infty} t[1 - F(t)] dt - HRT^2 \quad (8)$$

With:

$C(t)$ = the distribution curve with the concentration in function of the time

$F(t)$ = the cumulative distribution curve as function of time

σ^2 = the variance of the calculated HRT

3.4.2 Dry matter and volatile attached solids

The moisture content and volatile attached solids of the tested soil samples were measured using a thermal process. This process was carried out in duplicate for each sample with weight measurements executed 3x every step. This used methodology is based on EPAs method 1684 (EPA, 2001).

Furthermore, following steps were operated in order to obtain the necessary data:

- **W₀**: Aluminium discs were weighted on a tarred scale.
- **W₁**: This is followed by the addition of 25 – 50 g of humid soil on the discs which were then weighted again.

Thereafter the samples were dried for 6 hours at 105 °C in the electric drying oven.

- **W₂**: After cooling down in the desiccator and a third weight measurement, samples were put back in the oven for another 30 minutes at 105 °C.
- **W₃**: With a maximal permissible weight difference of 5 %, complete dehydration could be confirmed and values for the total dry matter could be calculated

If this limit was exceeded, another drying cycle of 0.5 - 1 hour at 105 °C was executed (**W_{3,new}** would be used then instead of **W₃**). This was repeated until the results were acceptable. Using the following equations the value for the dry matter (DM) was calculated.

$$DM = \frac{W_3 - W_0}{W_1 - W_0} \quad \left[\frac{g}{g} \right] \quad (9)$$

$$DM = \frac{W_3 - W_0}{W_1 - W_0} * 100 \quad [\%] \quad (10)$$

When proceeding for the volatile attached solids (VAS), the dried samples were placed in the muffle furnace for 2 hours at 550 °C. After the elapsed time the samples were submitted to an equal procedure as for the dry matter (DM). During this procedure masses W_4 and W_5 (similar to W_2 and W_3 respectively) were measured. With this data the volatile attached solids were calculated using equations (11), (12) and (13).

In addition, the exact weight of the complete soil sample used in the respirometer is measured before starting the respirometry test (W_{sample}). By multiplying this with equation (11) an idea could be formed of the total amount of biomass inside the reactor (total VAS in grams). V_{sample} equals the measured volume of the sample itself, so the total grams of VAS per volume of sample (VAS in g/L) was calculated.

$$VAS = \frac{W_3 - W_5}{W_3 - W_0} \quad \left[\frac{g}{g} \right] \quad (11)$$

$$VAS = \frac{W_3 - W_5}{W_3 - W_0} * \frac{W_{sample}}{V_{sample}} \quad \left[\frac{g}{L} \right] \quad (12)$$

$$VAS = \frac{W_3 - W_5}{W_3 - W_0} * 100 \quad [\%] \quad (13)$$

Chapter 4

Results and discussion

4. Results and discussion

- 4.1 Tracer tests and hydraulic retention time
- 4.2 Dry matter and volatile attached solids (biomass)
- 4.3 Respirograms and yield coefficients
- 4.4 Summary of results and discussion

4.1 Tracer tests and hydraulic retention time

From the measured conductivities through time a conversion was made to actual concentrations using a calibration curve. Via equation (6) an HRT-profile was constructed (figure 19). By integrating this profile through time the total surface area above the graph was calculated corresponding with the exact HRT of the system (equation 7).

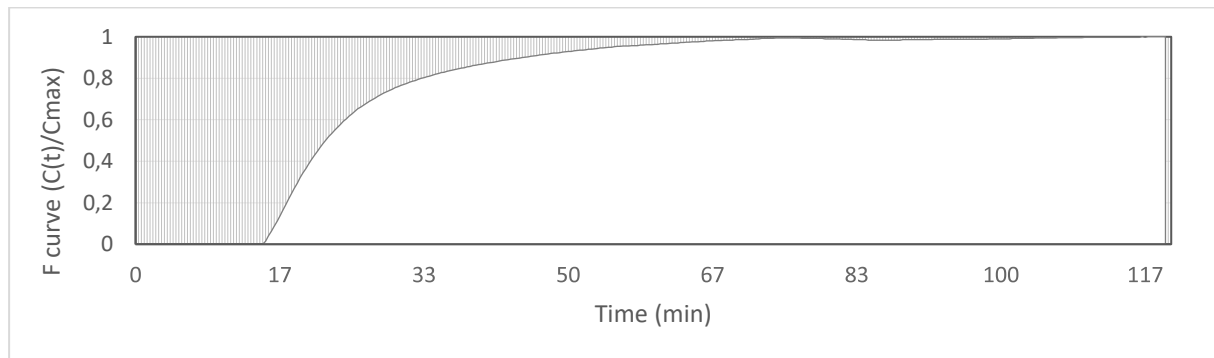


Figure 19: HRT profile for sample 1

A list of HRT-profiles of every sample is summarized in Appendix C: HRT-profiles for every sample.

From each sample, with exception of sample point no. 5, the hydraulic retention time was calculated in minutes and summarized in table 5 together with the standard deviation, σ (min). This was calculated by taking the square root of the results according to equation (8). At sample point no. 5, no HRT was measured due to the disability to start the system in the lab with water flowing through the sample. With every start, the respirometer immediately flooded because of clogging. Due to this result, an extra sample at point 4A was taken.

The results for the HRT are no exact measurements for the soil pore size distribution or the hydraulic pathways in the CW. A lot of differences could influence the results, making them not suitable for the comparison with the CW itself (stones, roots present, rainfall at the wetland etc.). Therefore, *in-situ* measurements of the hydraulic conductivity would help making comparing essential differences. Nevertheless it is used as an indicator for the hydraulic circumstances inside the wetland bed. A correlation between the HRT inside the respirometer and the hydraulic conductivity in the wetland is presumed. Because of the presence of two gravel layers inside the reactor, the HRT is expected to be influenced regarding the HRT for soil only. Gravel is assumed to cause a lower HRT which result in a small overestimation of it. In addition with this, the assumption that no oxygen is consumed between the first reading point and the start of the soil sample. This results to a slight underestimation of the calculated OUR.

Table 5: HRT and standard deviation of each sample

Sample point	HRT (min)	σ (min)	Sample point	HRT (min)	σ (min)
1	27	14	5	-	-
2	36	16	6	22	14
3	27	20	7	47	24
4	34	21	8	46	26
4A	53	36	9	47	30

The calculated values are represented in figure 20 with a 3D-chart. This map is no representation of the HRT through the wetland itself, but is an overview of the HRTs from the samples inside the respirometer, obtained from the corresponding places at the wetland. From this map, influent at the wetland arrives in front of point 2 (first row, centre), is distributed over the first row and leaves the CW right across the field (after row 3).

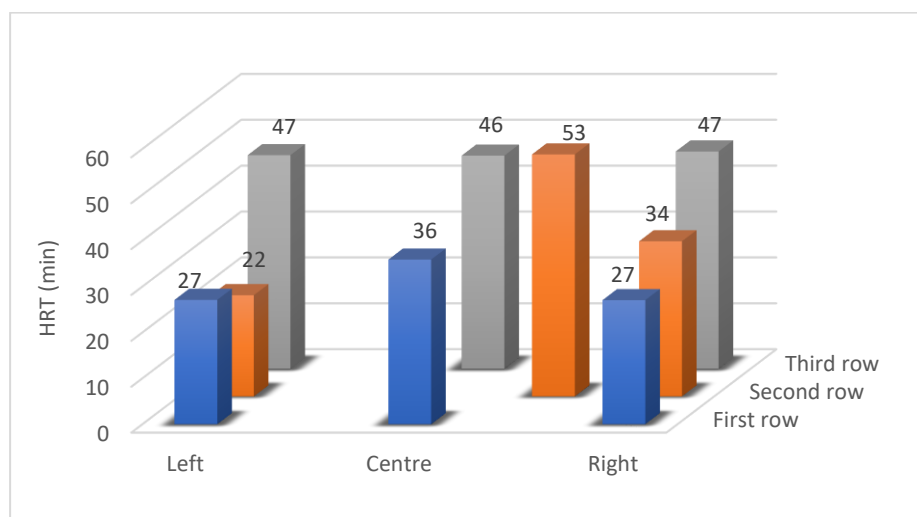


Figure 20: 3D overview of the HRT (min) of each sample according to the wetland position

Based on the measured HRT from samples at different points on the wetland, a hypothesis is developed to describe the water flow through the wetland. This plan is visualized in figure 21, with arrows indicating the differences in hydraulic flow paths across the land.

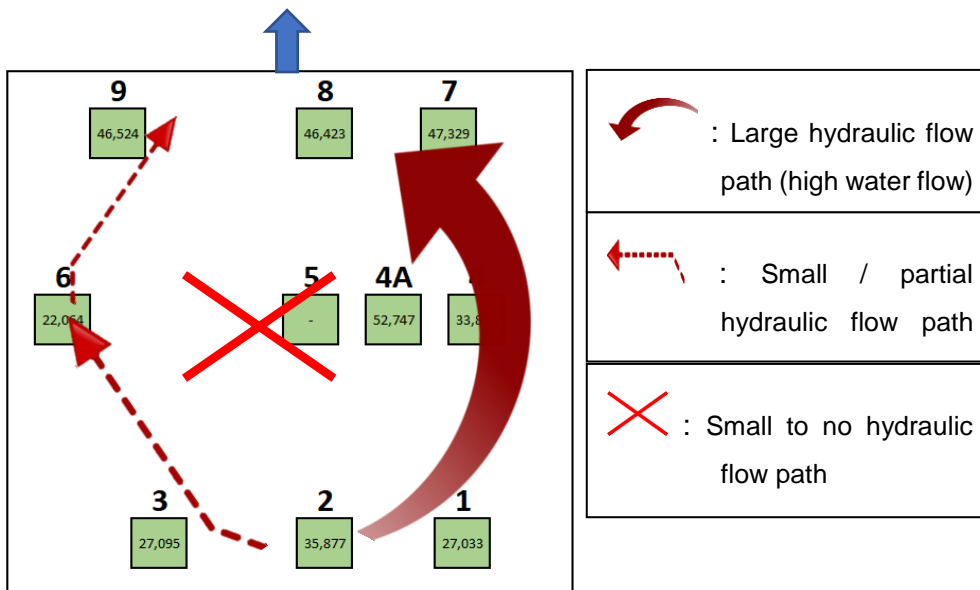


Figure 21: CW overview with the HRT (min) from each sample at the respirometer

The first row shows a rather constant value for the HRT indicating an equal pore size distribution of the soil and less preferential hydraulic path ways. The middle HRT (point 2: 36 min) is slightly higher, which could be caused by the higher flow rates immediately in front of the inlet. This leads to an higher amount of particles obstructing open pores at the inlet.

For **the second row**, no water could get through soil obtained from the absolute centre of the wetland because of its low porosity. Investigating the sides of the wetland, the right side (point 4: 34 min) showed a good flow and low HRT. When approaching more to the centre, HRT rises (point 4A: 53 min). At the left side (point 6) the tests encountered a lot of difficulties as the maximum (water) flow rate reached was 8-10 ml/min, which is too low to maintain a correct test. With the expectation of a high HRT, the result appears to be significant shorter compared to the others. However, this result is assumed to be incorrect, as the resulted HRT from other samples matched better with the expectations based on the flow rate during the respirometric tests.

Presumably the low HRT at point 6 (measured 22 min) is false due to measuring errors. These errors are in all probability caused by preferential flow paths from the water through the soil inside the reactor. As the result for the tracer tests only were calculated after the change of new sample, duplicate measurements for the HRT were not executed. This makes the detection of possible measuring errors more difficult. However, the test procedure for every sample was carried out as equal as possible, only the amount of soil used in the test could differ slightly just as the flow rate (taken into account) and the possible compression (compression was avoided as much as possible). Notwithstanding, sample 1 and 3 also show rather low HRTs. It is more assumable that these measurements are more correct because of the higher flow rate during the tests with these samples.

Predictions for possible clogged areas are difficult to perform. Reasons for the clogging could be the result of different loading rates, unequal pore size distribution, obstruction by accumulated solids and particles, excessive or different vegetation growing. For exact causes of the clogging further investigation of the specific areas should be executed.

The last row shows some unexpected results. Following the hypothesis a low HRT was expected more at the right hand side of the wetland (following the biggest flow path of water). The rising HRT from the beginning of the wetland to the end is consistent, but contradictory to the expectations. Typically with the wetland length, less solids are present in the water because of natural filtration. With a lower amount of solids, free pores are less obstructed so the water flow would be better (lower HRT). With these results we can assume a similar pore size distribution, or density as in sample point 4A. There appears to be no significant distinctions between the three rear points (± 47 min), so it is likely that no preferential flow path occurs at the last row.

At the last row, the more increasing HRT could be the result of higher vegetation growth or fewer hydraulic pathways. A more continuous (higher) loading rate, could contribute to provide a better flow through the complete wetland.

4.2 Dry matter and volatile attached solids (biomass)

According to equation (10) and (11) the dry matter content and volatile attached solids was determined. For the attached solids, the total weight of sample used in the respirometer and its volume were used to determine the total weight of VAS inside the reactor (in grams) and to determine the total amount of VAS in grams per litre sample.

For every sample, 4 to 8 different duplicates were measured to determine the DM and VAS. Within every set of duplicates for one sample, outliers were determined. These calculations were based on the method described by Weiss (2016) (section 3.3, pg. 115). The limits were determined using the equations mentioned below, so data with values lower or higher than this limit could be rejected.

$$\text{Lower limit} = Q_1 - 1.5 * \text{IQR}$$

$$\text{Upper limit} = Q_3 + 1.5 * \text{IQR}$$

With:

$Q_1 = 25^{\text{th}}$ percentile: the first 25% of the data when arranged from low to high

$Q_3 = 75^{\text{th}}$ percentile: the last 25% of the data when arranged from low to high

$$\text{IQR} = Q_3 - Q_1$$

This resulted in a data set for each sample without outliers. For every sample, this data set was used to calculate the average DM and VAS values as well as the standard deviation. These results are tabulated in table 6.

Table 6: Determined dry matter and volatile attached solids

Sample no.	Dry matter		W_{sample} (g)	V_{sample} (L)	VAS		VAS	
	DM (%)	σ (%)			VAS (g)	σ (g)	VAS (g/L)	σ (g/L)
1	70.73	1.82	768	0.610	27.120	2.318	44.459	3.800
2	61.62	7.01	931	0.510	66.985	41.013	131.343	80.419
3	69.39	3.06	982	0.600	28.698	1.576	47.830	2.626
4	63.56	2.97	865	0.600	73.141	34.780	121.901	57.967
4A	72.72	1.72	999	0.640	26.860	2.704	41.969	4.226
5	78.13	0.55	727	0.700	16.079	0.444	22.970	0.634
6	68.86	0.88	902	0.550	24.019	1.072	43.671	1.948
7	72.04	1.37	940	0.600	21.694	1.125	36.156	1.876
8	73.16	0.82	978	0.650	22.435	0.403	34.515	0.619
9	73.88	0.48	978	0.700	23.170	4.148	33.099	5.925

Values for the DM content show roughly similar values and are classified in the range of 61.62% to 78.13% with an average DM of 70.5% \pm 4.89%. These results depend mostly on the sample composition. Samples with a larger porosity, more organic matter or BM could induce different DM percentages. For sample 5 the lowest moisture content is measured (DM = 78.13%), which corresponds with the expectations as sample 5 clogged and would consist of a structure with a very low porosity (= less moist). Contrariwise, the results for point 2 (61.62%) and 4 (63.56%) contain the highest moisture content. This fit with the idea of a higher porosity or a higher retention of water due to a higher amount of organic matter at these points.

Using the overview in figure 22, the proposed model in “4.1 Tracer tests” for the hydraulic conductivity can be supported with the measured amount of VAS. Moving from the first row to the third one, the amount of VAS decreases gradually. This is presumably caused by the higher loading rates at the beginning of the CW (= more food), so more BM could be grown at those areas.

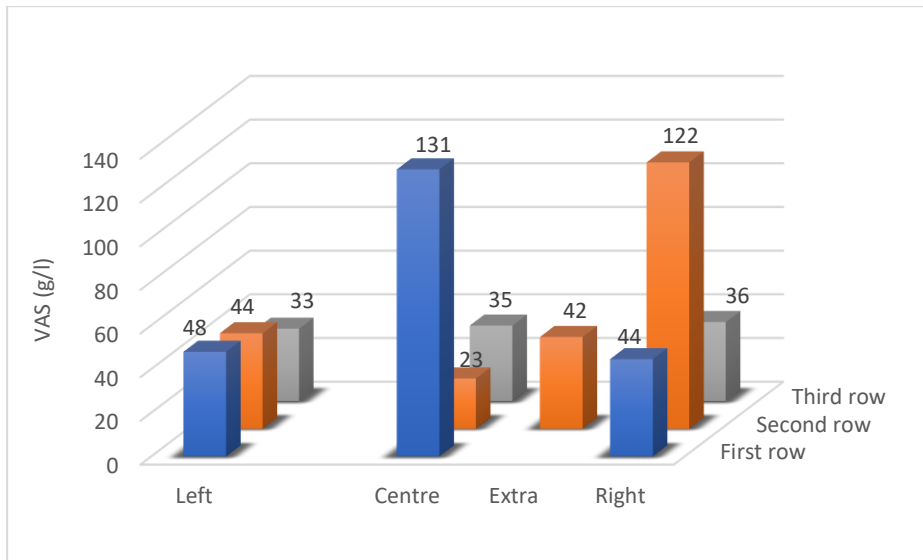


Figure 22: 3D overview of the VAS (g/L) of each sample according to the wetland position

In line with the assumed hydraulic flow path, the high values for the amount of attached solids at point 2 (131.340 g/L) and point 4 (121.901 g/L) support the hypothesis of a preferential flow path here. However, these two results do show a very large difference compared to the other points. The standard deviation also show a higher value. This is the result of measurements for sample 2 and 4 with a very differing outcome. Results for each sample are widely spread, as the highest measured VAS is more dan 2 times as big as the lowest measured VAS. Also the lower results for point 5 (22.970 g/L) could be explained by the low porosity, which result in less water flowing through that area, which brings a decreased food supply with it (= low MO growth). With approaching distance of the clogged zone, VAS decreases a lot.

In the last row a higher BM content would be expected at point 8 (34.515 g/L) because of its closest position with the outlet. In fact it differs not much from point 7 and 9 (36.156 g/L and 33.099 g/L respectively). So the amount of BM in the last row can be classified as more or less equal distributed. These low VAS concentration at the outlet could be the consequence of an adequate BOD-degradation efficiency at the start of the CW. Which results in the passage of more clean water with a low BOD contents in the last row. Data from effluent BOD-concentrations (Appendix B) could support this theory. However, the reduced VAS concentration would lead to more free spaces at the soils' pores, leading to a lower HRT. Further examination of the soil composition, hydraulic conductivity, vegetation growth, presence of solids and biomass... is needed to explain the unexpected results for the HRT at the end of the wetland bed.

Important to mention is the overestimation made for the amount of BM present in the samples. During these tests, all parts of leaves, little stones, organic material and roots are filtered out as much as possible. Unavoidably a part of these interferences will stay present in the soil, which will result in an error for the VAS results and an overestimation of the exact amount of micro-organisms (biomass) present in the reactor during the tests.

4.3 Respirograms and yield coefficients

From the respirometry tests and the measured DO-profiles, various respirograms were obtained. In every chart, two signals are displayed. Both respirograms should contribute to the same result. Following legend is used to clarify the differences:

-  OUR profile without temperature correction
-  OUR profile with temperature correction
-  Marks for the beginning, acetate depletion and ending of the test²
-  Level of endogenous respiration⁴

For every test a different type of respirogram is classified according to the proposed models of Piseiro *et al.* (2017). Different yield values for the BM growth and storage growth are compared, together with the consistency during consecutive tests and between the different sample points at the CW. The average temperature of the circulating water during the tests is added. This showed no large fluctuations, further discussion is included in “4.4.1”.

Note that there appears to be a small time shift between both profiles. This has actually no biochemical meaning, but is just a pure mathematical consequence of the correction made during calculations.

² Based on the OUR profile without temperature correction in order to have a better visual for the critical points.

Sample 1

Soil from sampling point no. 1 was obtained at 12/10/2018. At every performed test a typical **respirogram** type I is observed. During the tests the amount of **feeding (S_s)** varies slightly, although the aim to add a concentration of 30 – 50 mg COD/L approximately, a lower feeding was handled. This is due to a wrong estimation, as it were the first tests. Different **maximum peak heights** of $\pm 8 - 13 - 12$ mg $O_2/L/h$ were observed, proportional to the added acetate concentration. Levels for **endogenous respiration** are nearly constant (respectively 3-4 mg $O_2/L/h$). Averages for both yield values Y_H and Y_{STO} are 0.885 mg COD/mg COD. Only the first test showed higher yield values, while the yields in test 2 and 3 are more constant.

During the last test, **nitrification** occurred inside the reactor (figure 26). This appearance is not exceptional, although it only appeared in this one test (compared to all tests across the thesis). Presumable ideal circumstances happened in certain zones of the reactor, e.g. anaerobic conditions, so the nitrifying bacteria present in the soil sample could grow throughout the different test and eventually, start the nitrification process. Hence, the coefficient results from the last tests are excluded in the average result for sample 1.

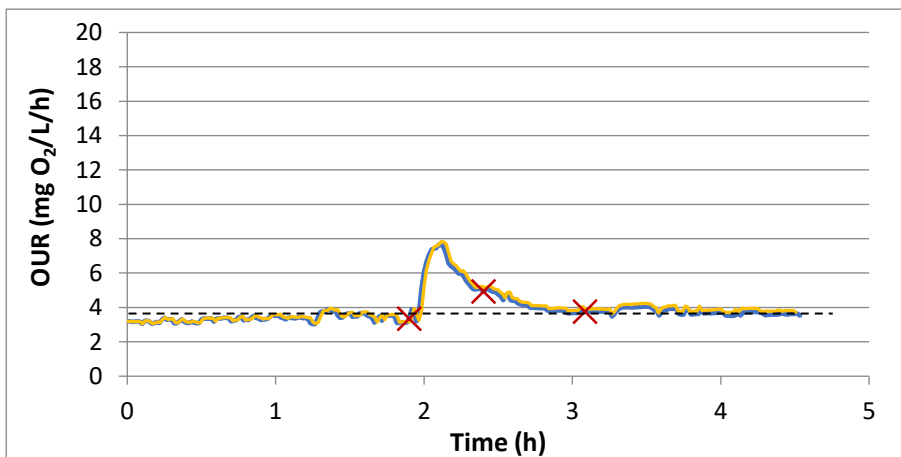


Figure 23: Respirogram and stoichiometric results sample 1, test 1 (26/10/2018)

Type	I
S_s (mg/L)	11.532
Y_H (mg COD/ mg COD)	0.926
Y_{STO} (mg COD/ mg COD)	0.938
T_{av} ($^{\circ}C$)	19.73

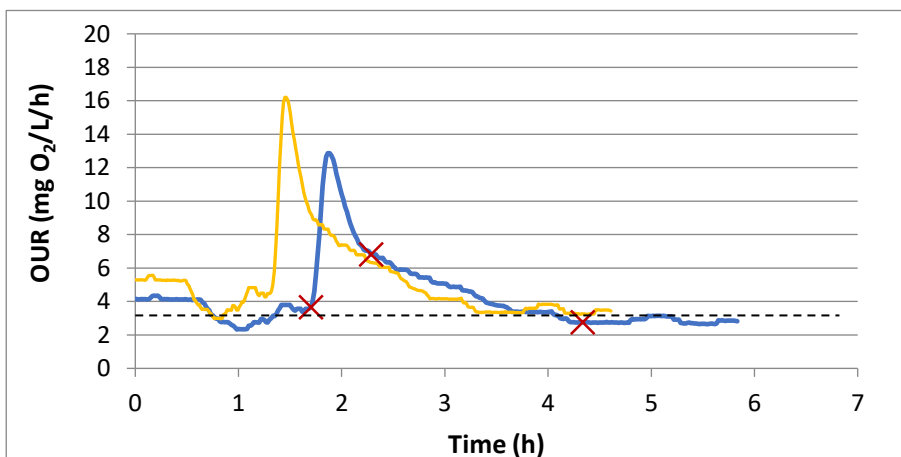


Figure 24: Respirogram and stoichiometric results sample 1, test 2 (29/10/2018)

Type	I
S_s (mg/L)	19.220
Y_H (mg COD/ mg COD)	0.885
Y_{STO} (mg COD/ mg COD)	0.806
T_{av} ($^{\circ}C$)	17.12

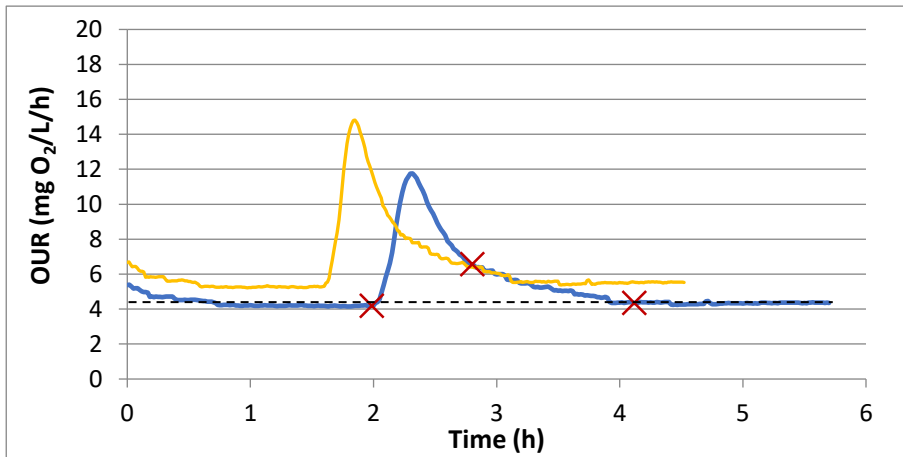


Figure 25: Respirogram and stoichiometric results sample 1, test 3 (30/10/2018)

Type	I
S _s (mg/L)	15.376
Y _H (mg COD/ mg COD)	0.843
Y _{STO} (mg COD/ mg COD)	0.860
T _{av} (°C)	16.92

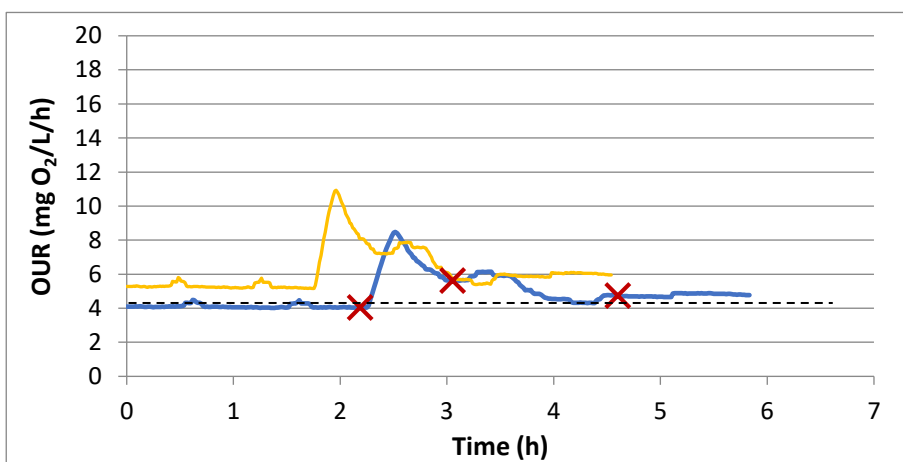


Figure 26: Respirogram and stoichiometric results sample 1, test 4 (31/10/2018)

Type	I
S _s (mg/L)	15.376
Y _H (mg COD/ mg COD)	0.911
Y _{STO} (mg COD/ mg COD)	0.900
T _{av} (°C)	16.98

Sample 2

Samples at the inlet (point no. 2) were obtained the 9th of November 2018. During the tests all three respirograms show a clear **type III** graph. This result corresponds with the research of Piseiro *et al.* (2017) where these type of respirograms are expected from samples subjected to high loading rates. For these types, storage is expected to be low or null, which matches with the results. Nevertheless, the Y_{STO}, maximum OUR and duration of the substrate consumption decreases with time (and additional tests). This could be the result of rather low loading rates during the tests, compared to the high loading rate at the wetland. Values for Y_H show fluctuating results, with no explicit correlation. During the first test a negative value is obtained (-0.449), meaning more oxygen is consumed than added. This could be the result of settled biomass in the measuring cell. Therefore this result is excluded in the average yield result. **Endogenous respiration** levels are measured around 8 – 9 mg O₂/L/h and **maximum OUR-values** of 20, 21 and 17 mg O₂/L/h. The time to oxidize all the substrate is longer compared to other samples (+ 4h).

For the second test a significant higher concentration of substrate is added. This is due to the change of sodium acetate solution. The new solution (2909 mg COD/L), compared to the first solution used (961 mg COD/L), had a much higher concentration. This large change in **feeding** was corrected in the third test of sample 2.

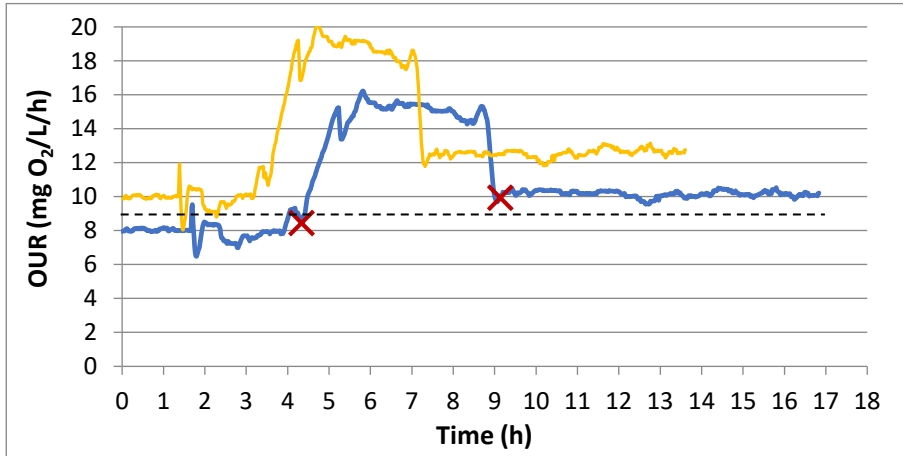


Figure 27: Respirogram and stoichiometric results sample 2, test 1 (11/11/2018)

Type	III
S _s (mg/L)	16.818
Y _H (mg COD/ mg COD)	-0.449
Y _{STO} (mg COD/ mg COD)	-
T _{av} (°C)	17.22

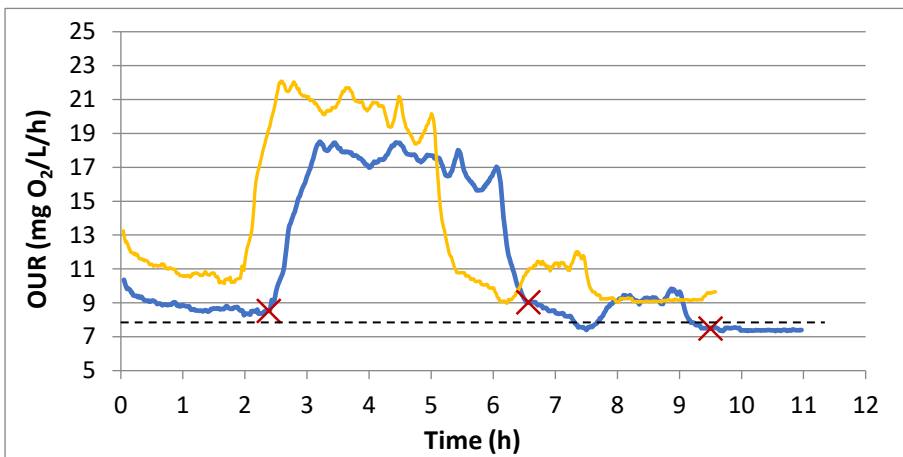


Figure 28: Respirogram and stoichiometric results sample 2, test 2 (13/11/2018)

Type	III
S _s (mg/L)	59.500
Y _H (mg COD/ mg COD)	0.493
Y _{STO} (mg COD/ mg COD)	0.917
T _{av} (°C)	17.42

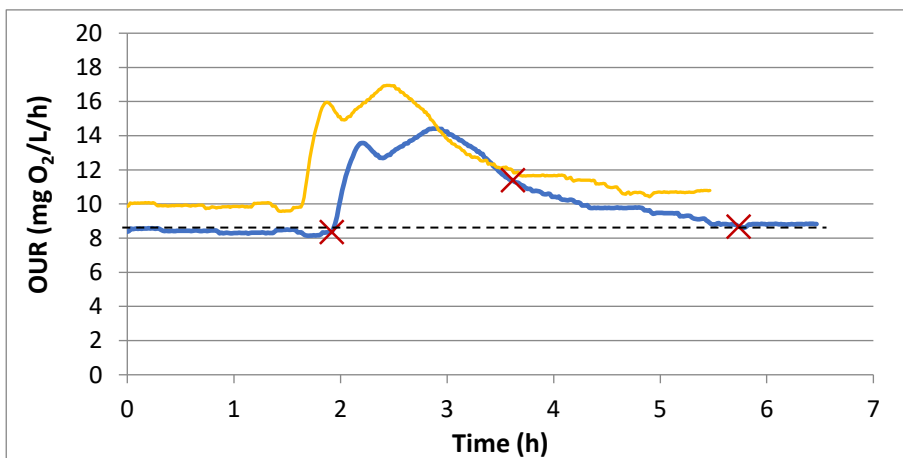
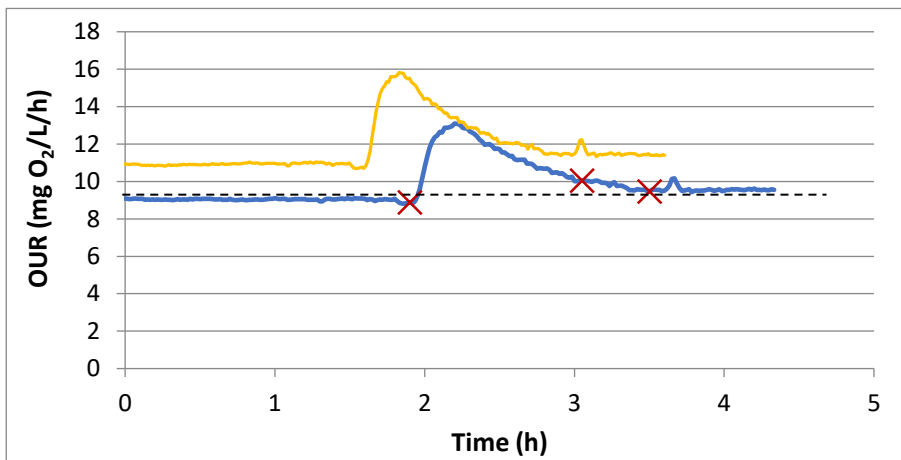


Figure 29: Respirogram and stoichiometric results sample 2, test 3 (14/11/2018)

Type	III
S _s (mg/L)	22.313
Y _H (mg COD/ mg COD)	0.764
Y _{STO} (mg COD/ mg COD)	0.777
T _{av} (°C)	17.73

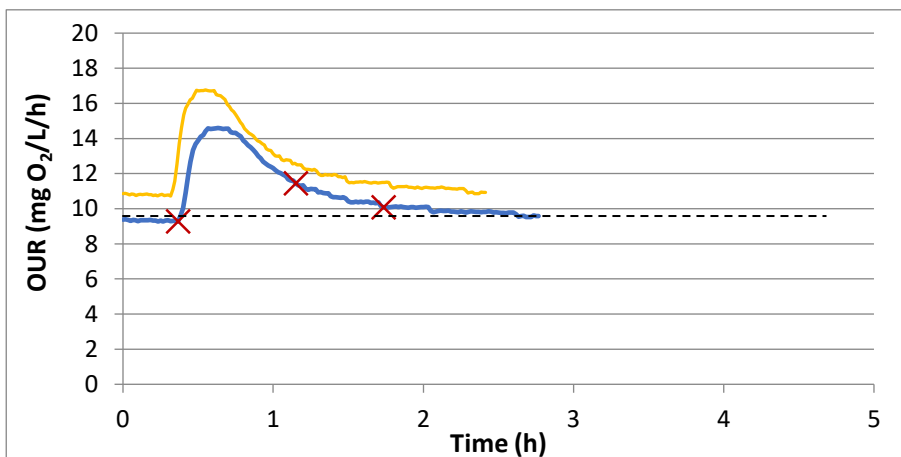
Sample 3

Sample 3 was retrieved on 15/11/2018. Tests from this sample showed results similar to the ones from sample 1 with all **type I** respirograms. Nevertheless the OUR-peaks are less sharp, but higher around 13 – 14 – 16 mg O₂/L/h. **Endogenous respiration** level is constant (± 9 mg O₂/L/h) and the **durations** for the substrate oxidations are 1.5 – 2 hours. **Substrate concentrations** (S_S) were increased in order to maintain a clear response from the samples MO. **Maximum peak heights** up to 16 mg O₂/L/h are less proportional to the feeding as a difference of 1.5-2 mg O₂/L/h is measured between test 2 and 3 (same S_S-concentration). Average values for Y_H and Y_{STO} are respectively 0.938 and 0.968 mg COD/mg COD.



Type	I
S _S (mg/L)	22.313
Y _H (mg COD/ mg COD)	0.902
Y _{STO} (mg COD/ mg COD)	0.973
T _{av} (°C)	17.62

Figure 30: Respirogram and stoichiometric results sample 3, test 1 (18/11/2018)



Type	I
S _S (mg/L)	37.188
Y _H (mg COD/ mg COD)	0.942
Y _{STO} (mg COD/ mg COD)	0.970
T _{av} (°C)	18.21

Figure 31: Respirogram and stoichiometric results sample 3, test 2 (19/11/2018)

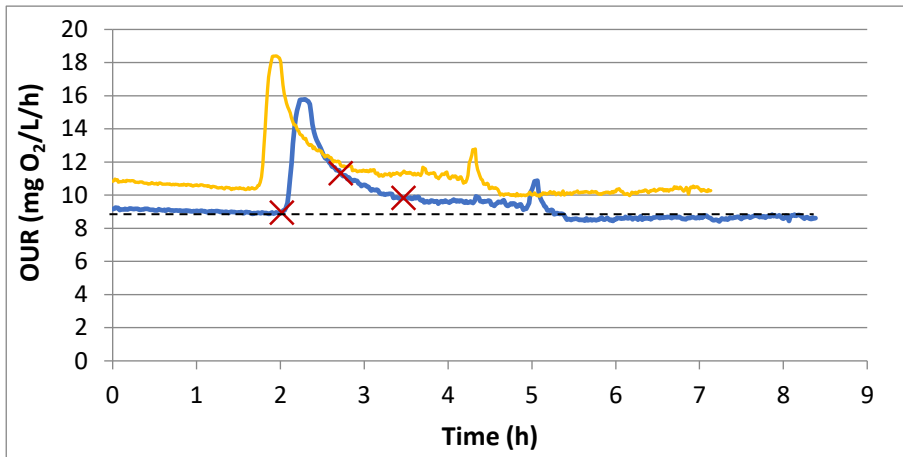


Figure 32: Respirogram and stoichiometric results sample 3, test 3 (20/11/2018)

Type	I
S _s (mg/L)	37.188
Y _H (mg COD/ mg COD)	0.948
Y _{STO} (mg COD/ mg COD)	0.965
T _{av} (°C)	17.88

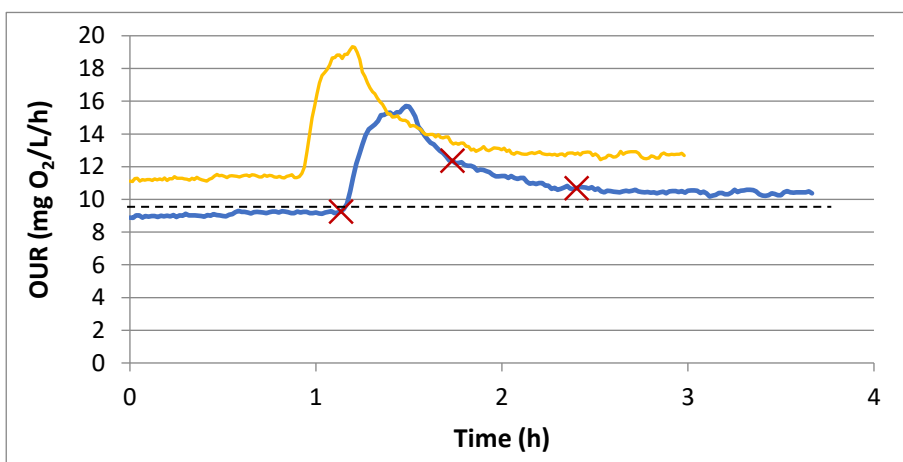


Figure 33: Respirogram and stoichiometric results sample 3, test 4 (21/11/2018)

Type	I
S _s (mg/L)	40.906
Y _H (mg COD/ mg COD)	0.958
Y _{STO} (mg COD/ mg COD)	0.965
T _{av} (°C)	17.29

Sample 4

The 30th of November 2018, soil from sample point 4 was collected. Tests with longer **durations** of 2.5 to 4 hours all resulted in **type I** respirograms. Despite the equal **feeding** of 31.6 mg/L for every tests, different peak heights were obtained. The first two tests reached a **maximum OUR** of 12 mg O₂/L/h while the third tests resulted in a maximum up to 16 mg O₂/L/h. For this higher peak height, the level of **endogenous respiration** also rises from 6 to 11 mg O₂/L/h. Concerning the yield values, both Y_H and Y_{STO} increase with additional tests. Average values are: Y_H = 0.929 mg COD/mg COD and Y_{STO} = 0.933 mg COD/mg COD.

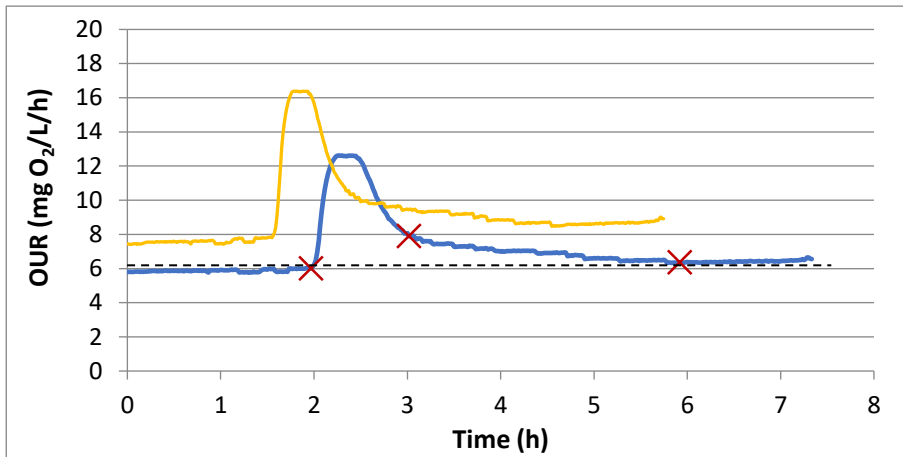


Figure 34: Respirogram and stoichiometric results sample 4, test 1 (6/12/2018)

Type	I
S _s (mg/L)	31.620
Y _H (mg COD/ mg COD)	0.887
Y _{STO} (mg COD/ mg COD)	0.906
T _{av} (°C)	16.45

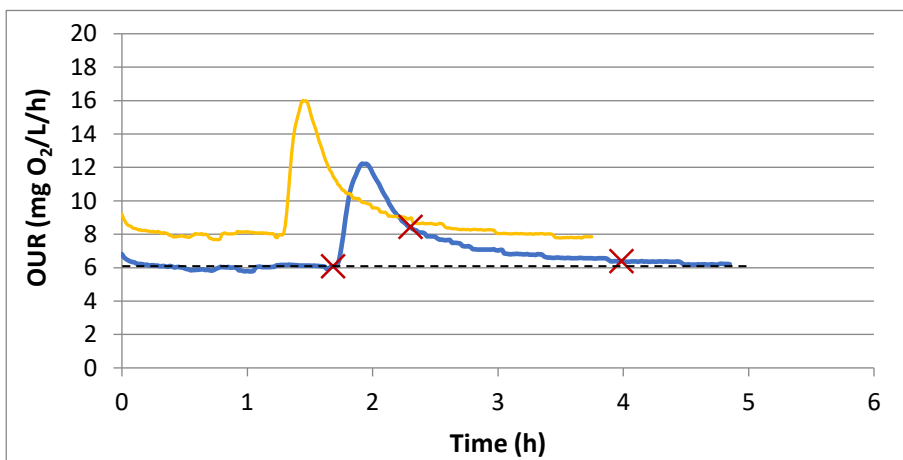


Figure 35: Respirogram and stoichiometric results sample 4, test 2 (7/12/2018)

Type	I
S _s (mg/L)	31.620
Y _H (mg COD/ mg COD)	0.948
Y _{STO} (mg COD/ mg COD)	0.938
T _{av} (°C)	16.61

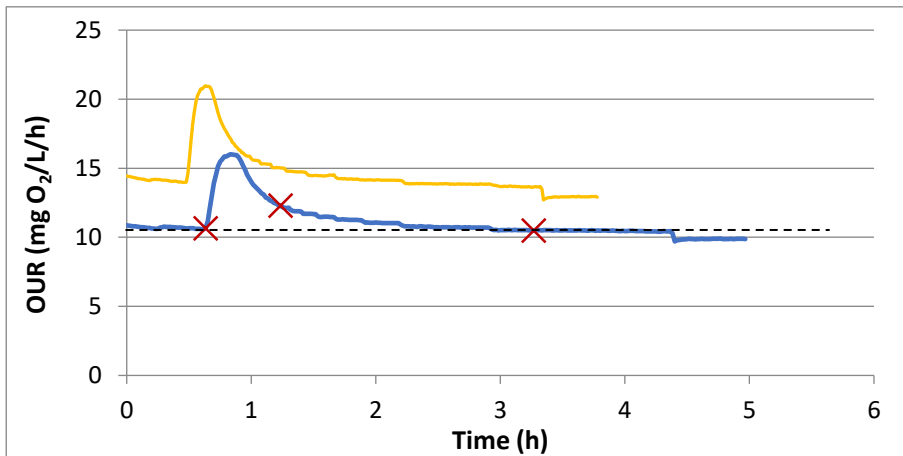


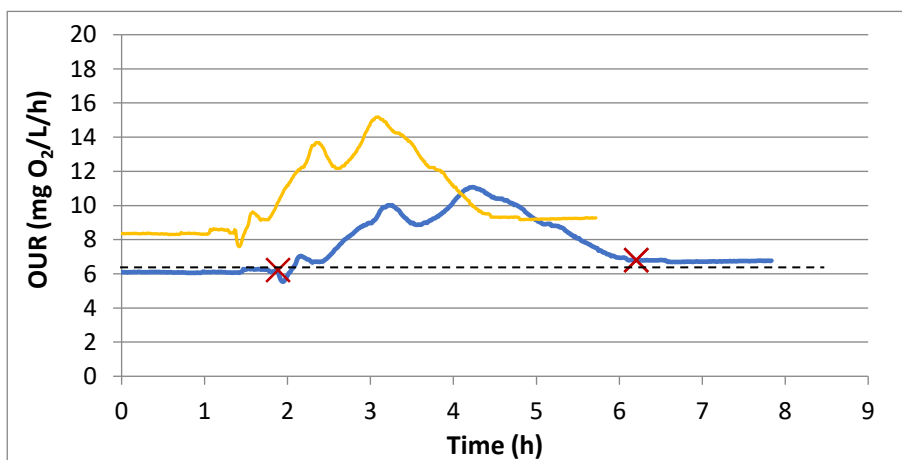
Figure 36: Respirogram and stoichiometric results sample 4, test 3 (9/12/2018)

Type	I
S _s (mg/L)	31.620
Y _H (mg COD/ mg COD)	0.951
Y _{STO} (mg COD/ mg COD)	0.954
T _{av} (°C)	16.17

Sample 4A

Sample 4A was retrieved together with the sample 4 at 30/11/2018. Sample 4A is the first sample where respirogram **type II** is observed. This type may be correlated to the HRT. As earlier mentioned, the larger HRT at sample 4A indicated a more dense soil structure, closer to the clogged area. For the different values of the tests with a constant **substrate concentration** of 36.4 mg/L (except test 1), fluctuating results are obtained. **Maximum OUR** peak heights differ from 11 to 8, 10 and 11 mg O₂/L/h again, with **durations** longer than 4 hours. This last parameter could be a characteristic of the type II OUR profile. Remarkable is that higher maximum OUR-values correspond with longer test durations. **Endogenous respiration** level from 6.5 mg O₂/L/h to 3.5-4 mg O₂/L/h.

Growth yield values Y_H fluctuated for every test, with an average $Y_H = 0.769$ mg COD/mg COD. For the storage mechanism another possible characteristic for type II respirogram is the absence of storage products. This was perceived during the first two tests. For test 3 and 4 the amount of storage products were growing with additional tests. The average $Y_{STO} = 0.794$ mg COD/mg COD. Assumably the sample from point 4A must be accustomed to a loading rate high enough to minimize storage formation, during the tests in the lab the low feeding patterns could activate the storage mechanism.



Type	II
S _s (mg/L)	29.090
Y _H (mg COD/ mg COD)	0.683
Y _{STO} (mg COD/ mg COD)	-
T _{av} (°C)	15.84

Figure 37: Respirogram and stoichiometric results sample 4A, test 1 (2/12/2018)

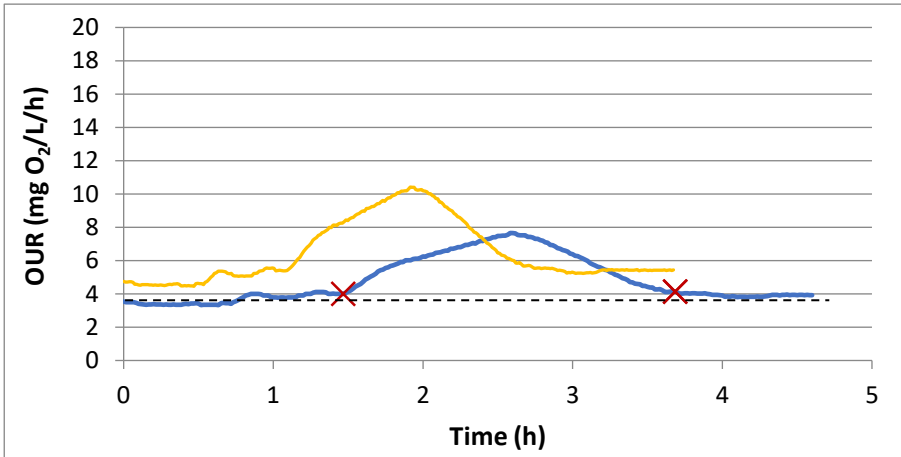


Figure 38: Respirogram and stoichiometric results sample 4A, test 2 (3/12/2018)

Type	II
S _s (mg/L)	36.363
Y _H (mg COD/ mg COD)	0.882
Y _{STO} (mg COD/ mg COD)	-
T _{av} (°C)	15.99

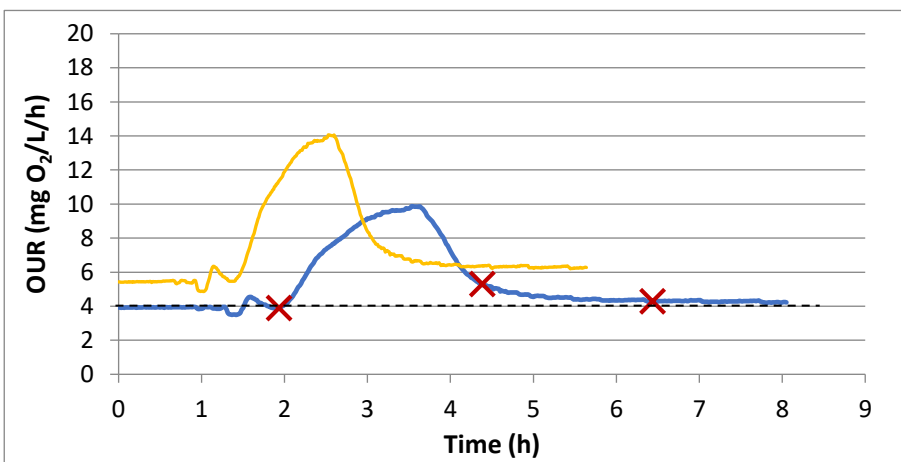


Figure 39: Respirogram and stoichiometric results sample 4A, test 3 (3/12/2018)

Type	II
S _s (mg/L)	36.363
Y _H (mg COD/ mg COD)	0.792
Y _{STO} (mg COD/ mg COD)	0.940
T _{av} (°C)	15.19

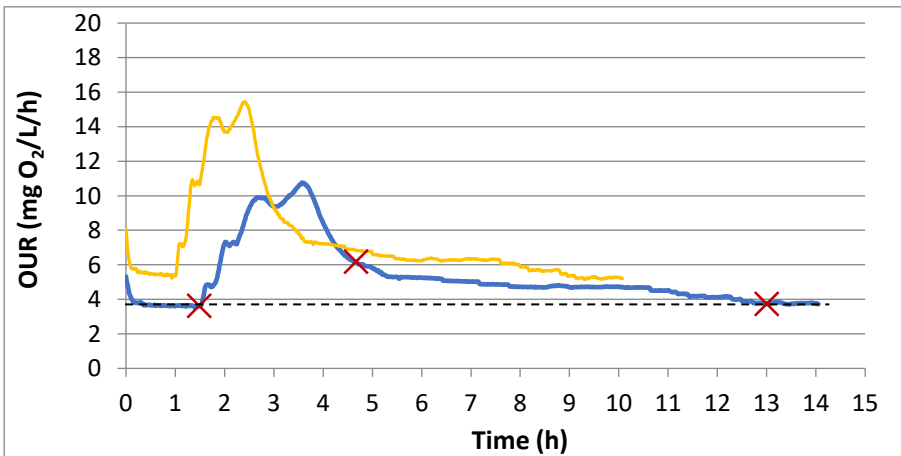


Figure 40: Respirogram and stoichiometric results sample 4A, test 4 (4/12/2018)

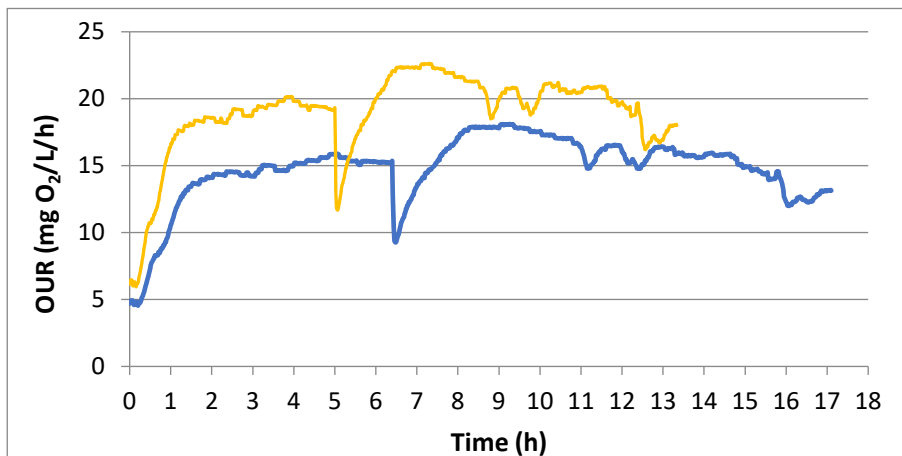
Type	II / III
S _s (mg/L)	36.363
Y _H (mg COD/ mg COD)	0.717
Y _{STO} (mg COD/ mg COD)	0.648
T _{av} (°C)	15.48

Sample 5

The sample from the fifth point at the wetland was collected the 26th of November 2018. Due to difficulties using soil from sample point no. 5, no measurements for respirometry could be obtained.

Sample 6

Sample 6 was retrieved on 10/12/2018. For tests with this sample, no useful data could be obtained. Beginning with the very low flow rate of water in the system, the signal of the DO-concentration did not reach an equilibrium. Based on the deviant HRT, a lot of preferential flow paths were present in the reactor leading to the fluctuating responses. Even with addition of substrate, unusual results were obtained leaving this sample with no stoichiometric values.



Type	-
S _s (mg/L)	14.545
Y _H (mg COD/ mg COD)	-
Y _{STO} (mg COD/ mg COD)	-
T _{av} (°C)	16.74

Figure 41: Respirogram and stoichiometric results sample 6 (12/12/2018)

Sample 7

Sample 7 was obtained together with sample 6 on 10/12/2018. Only with sample 4A and 7 respirogram **type II** was obtained. With constant **substrate concentration** (30.3 mg/L) **duration** times of 1.5 – 2.5 hours, **endogenous respiration** level of 7 – 8 mg O₂/L/h and **maximum peak heights** of 10 and 12 mg O₂/L/h were observed. Differently to sample 4A, storage products were already formed with the first test but were absent in the second one. Presumably the soil at point 7 has similar circumstances and density of soil from point 4A at the CW. The HRT is only 5 min shorter for sample 7, it has both type II respirogram and less storage to no storage products. Therefore the hypothesis developed in “4.1 Tracer tests” needs to be adjusted with the possibility of low hydraulic activity around point 7 (similar as point 4A).

Important to note with tests from sample 7 is that remarkably lower responses and peaks are observed. This made it more difficult to determine the exact start, middle and end of the tests as these marks are visually specified. The chance of errors will increase with less clear OUR-profiles (and lower accuracies). Values for the yield coefficients were constant with averages of $Y_H = 0.961$ mg COD/mg COD and $Y_{STO} = 0.962$ mg COD/mg COD.

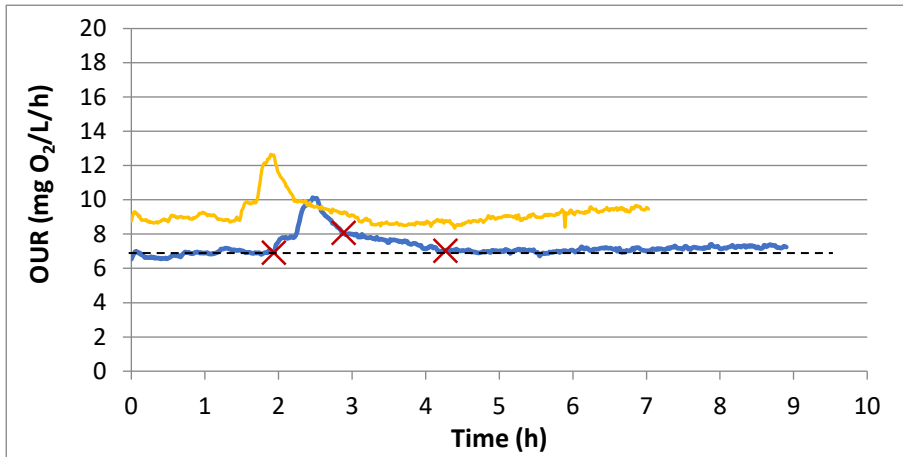


Figure 42: Respirogram and stoichiometric results sample 7, test 1 (18/12/2018)

Type	II
S_s (mg/L)	30.302
Y_H (mg COD/ mg COD)	0.963
Y_{STO} (mg COD/ mg COD)	0.956
T_{av} (°C)	16.81

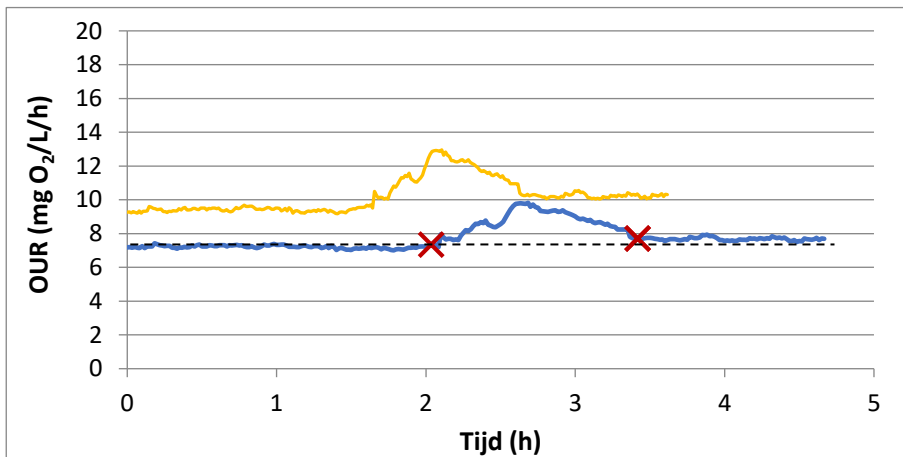


Figure 43: Respirogram and stoichiometric results sample 7, test 2 (18/12/2018)

Type	II
S_s (mg/L)	30.302
Y_H (mg COD/ mg COD)	0.948
Y_{STO} (mg COD/ mg COD)	-
T_{av} (°C)	16.38

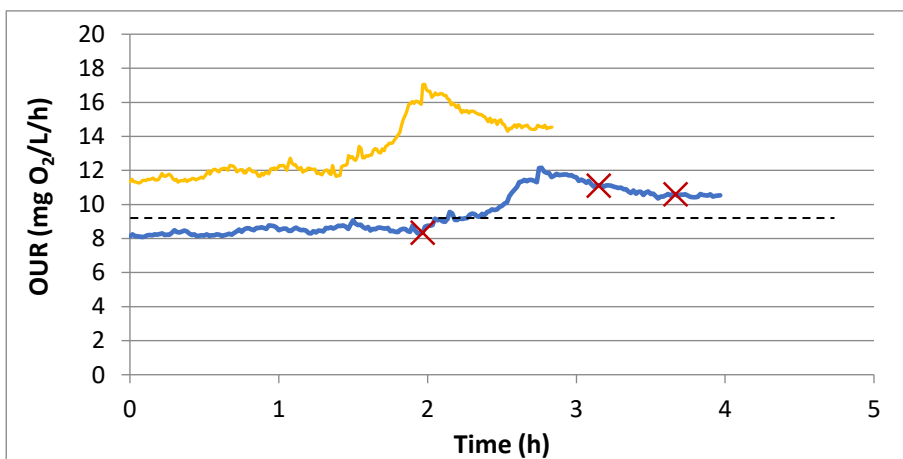


Figure 44: Respirogram and stoichiometric results sample 7, test 3 (19/12/2018)

Type	II
S_s (mg/L)	30.302
Y_H (mg COD/ mg COD)	0.972
Y_{STO} (mg COD/ mg COD)	0.968
T_{av} (°C)	15.71

Sample 8

The sample at the outlet (point 8) was collected the 14th of January 2019. For this sample, again **type III** respirograms were measured, similar as sample 2 (from the inlet of the CW). A constant **feeding** of 32.3 mg/L was added and resulted in three respirograms with **endogenous respiration** level between 2 and 3 mg O₂/L/h and **maximum OUR-values** of 10 mg O₂/L/h. One of the big differences compared to sample 2 is the long **duration** of the tests (up to 6 hours or more). This could be explained if the HRT of sample 2 and 8 are compared (respectively ± 35 min and. ± 46 min). Following this HRT the soil at point 8 must be more dense, which is contradictory to the type III respirograms for samples used to high loading rates.

Values for both yield coefficient differ a lot with decreases of 0.350 mg COD/mg COD over 3 tests. An average value for $Y_H = 0.324$ mg COD/mg COD, which is significantly lower than results from sample 2. In line with sample 2, only small amounts of storage products were observed. The slightly higher Y_{STO} (average 0.875 mg COD/mg COD) is probably caused by the lower loading rate, so MO are less used to be constantly loaded with nutritions.

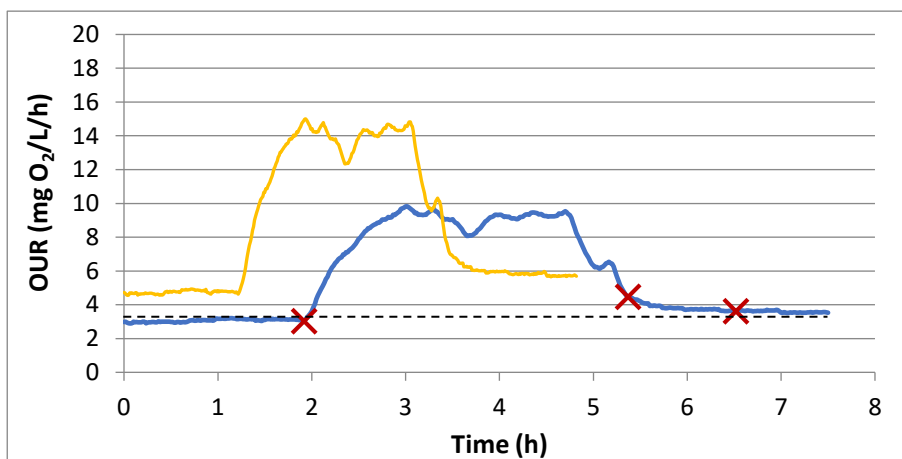


Figure 45: Respirogram and stoichiometric results sample 8, test 1 (17/01/2019)

Type	III
S _s (mg/L)	32.322
Y _H (mg COD/ mg COD)	0.537
Y _{STO} (mg COD/ mg COD)	0.936
T _{av} (°C)	14.14

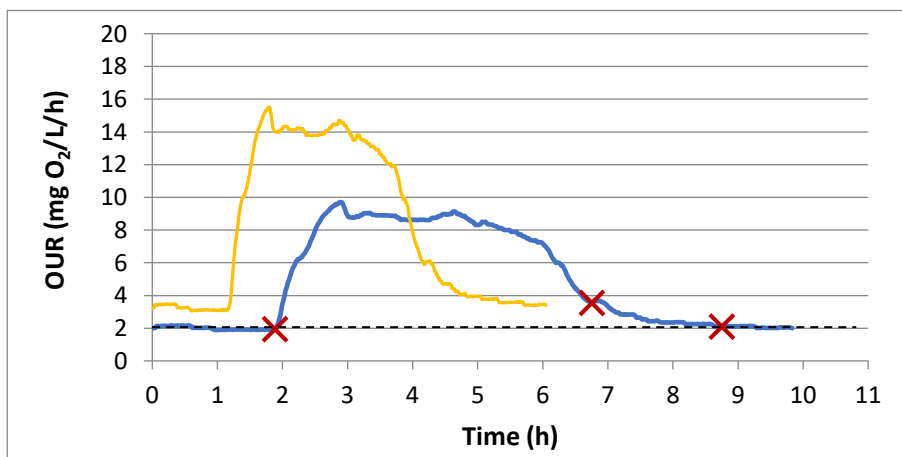
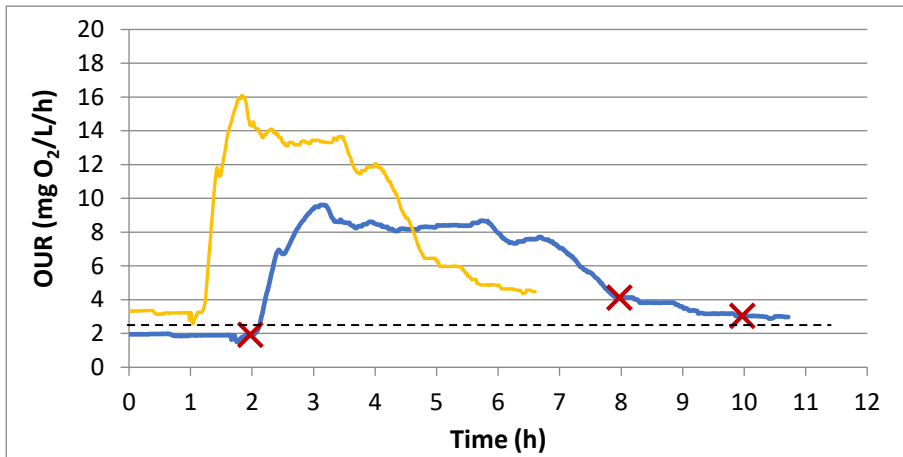


Figure 46: Respirogram and stoichiometric results sample 8, test 2 (17/01/2019)

Type	III
S _s (mg/L)	32.322
Y _H (mg COD/ mg COD)	0.259
Y _{STO} (mg COD/ mg COD)	0.855
T _{av} (°C)	13.56

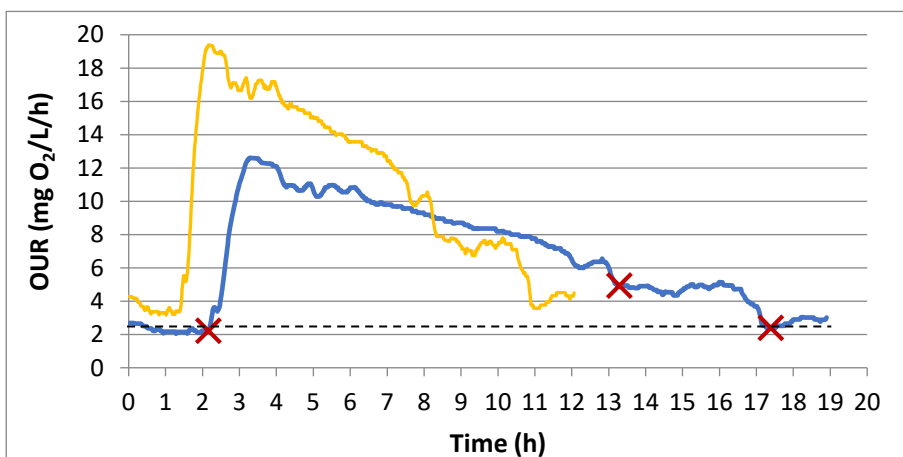


Type	III
S _s (mg/L)	32.322
Y _H (mg COD/ mg COD)	0.175
Y _{STO} (mg COD/ mg COD)	0.833
T _{av} (°C)	13.79

Figure 47: Respirogram and stoichiometric results sample 8, test 3 (18/01/2019)

Sample 9

The last sample was collected together with sample 8 on the 14th of January 2019. For this sample one test was executed resulting in a **type I** profile which was measured during a test of more than 10 hours. This long **duration** is mainly due to the very low flow rate of the water in the respirometer during the test. This is in line with the hypothesis earlier mentioned about the hydraulic flow paths inside the wetland causing a part of the wetland to be drier. Together with the flow rate, settling of BM inside the measuring cell caused the result to be overestimated. Therefore, the negative Y_H: -1.204 mg COD/mg COD and Y_{STO} = 0.136 are neglected as quantitative results for the summary of results.



Type	I
S _s (mg/L)	26.935
Y _H (mg COD/ mg COD)	-1.204
Y _{STO} (mg COD/ mg COD)	0.136
T _{av} (°C)	14.17

Figure 48: Respirogram and stoichiometric results sample 9, test 1 (20/01/2019)

4.4 Summary of results and discussion

4.4.1 Summary of parameters and their correlation

Table 7 gives an overview of the Y_H and Y_{STO} averages together with the feeding, VAS and F:M ratios, type respirogram and maximum peak height of the OUR-profile (sample 5, 6 and 9 excluded). The F:M-ratio is calculated by following equation in order to obtain a more comparable parameter and possibly clear correlation:

$$F:M \left(\frac{mg}{g}\right) = \frac{\text{Feeding} * \text{volume water}}{\text{Biomass present}} = \frac{S_s \left(\frac{mg}{L}\right) * V_{\text{water in reactor}}(L)}{VAS (g)}$$

Table 7: Summary of the stoichiometric results and F:M ratios

	Y_H (mg COD /mg COD)	Y_{STO} (mg COD /mg COD)	$S_s * V$ (mg)	VAS (g)	F:M (mg/g)	Type	Max OUR (mg O ₂ /L/h)
Sample 1	0.885	0.885	3.84	27.120	0.14	I	± 11
Sample 2	0.629	0.847	6.58	66.985	0.10	III	± 19.5
Sample 3	0.938	0.968	6.88	28.698	0.24	I	± 15
Sample 4	0.929	0.933	7.27	73.141	0.10	I	± 13.3
Sample 4A	0.769	0.794	6.91	26.860	0.26	II	± 10
Sample 7	0.961	0.962	7.27	21.694	0.34	II	± 10.6
Sample 8	0.324	0.875	7.27	22.435	0.32	III	± 10

Table 7 and table 8, summarize different parameters / characteristics. From the data for every test, regression analysis was used to detect possible correlations between the parameters. Some results showed a significant correlation (p-value < 0.05), but were followed by a really low adjusted R²-value (all with R² << 0,5). Meaning only weak relationships could be concluded. The following parameters indicated positive results:

- The maximum OUR peak height (mg O₂/L/h) and the VAS (g/L) show a very weak (but significant) correlation with an adjusted R² value of **0.32**. Especially because both parameters also depend on the provided substrate concentration (and with the F:M-ratio). However, the correlation corresponds with a logical expectation where a higher amount of MO would cause a higher oxygen consumption rate, or more available food causing higher peaks for the consumption rate..

- Maximum OUR peak height and the HRT ($R^2_{adj} = \mathbf{0.28}$). Different HRT results could indicate different circumstances inside the soil: aerobic/anaerobic circumstances influencing the aerobic oxidation reaction, the time for MO to consume the added substrate... These factors could motivate a changing OUR peak height.
- The level of endogenous respiration with the amount of VAS ($R^2_{adj} = \mathbf{0.12}$), the HRT ($R^2_{adj} = \mathbf{0.13}$) or the duration of the tests ($R^2_{adj} = \mathbf{0.15}$). The relationship between these parameters is explainable, although the correlation is very weak. With fewer microorganisms, endogenous respiration could be lower (lower growth and decay rate), which also influences the duration before all substrate is consumed. Regarding the HRT, a similar assumption for its influence is assumed as explained above.
- The temperature with the HRT ($R^2_{adj} = \mathbf{0.48}$), duration ($R^2_{adj} = \mathbf{0.28}$) or maximum OUR peak height ($R^2_{adj} = \mathbf{0.12}$). As explained in the literature, the temperature can affect the microorganisms kinetics, and microbiological activity. If the average temperature rises, MO will have more kinetic energy to consume the substrate causing the peak height to increase and to shorten the test duration.

One of the best correlations obtained is the temperature with the HRT. This is more unexpected and difficult to explain. The temperature variations are too small to cause particles to expand and obstruct the water flow or to cause a significant difference in viscosity. Further research would be needed to determine the possible coincidence of this correlation.

- Y_H and the tests duration ($R^2_{adj} = \mathbf{0.29}$). An explanation for this link could be the difference in F:M ratio which influences the duration (more food with less MO will take longer to oxidize all the substrate). So in an indirect way, the Y_H and duration are also correlated.
- Y_{STO} and the HRT ($R^2_{adj} = \mathbf{0.17}$). This correlation seems less plausible. An explanation for this possible correlation could be that a higher HRT leads to more anaerobic zones which decreases the aerobic (storage) growth yield. Although statistically not confirmed, the influence of the HRT on Y_H would be expected for the similar reasons as the HRT and Y_{STO} .

Better correlations were expected between different characteristics. Especially for factors as a higher amount of MO causing more cell growth and decay. This could be linked with the F:M-ratio, Y_H , Y_{STO} , endogenous respiration and other parameters. With higher HRT, water possibly endures more difficulties when migrating through the soil, which can increase the test duration (substrate will be divided slower). Even with the coherent explanation for these possible correlations, the results still showed a very weak correlation to conclude a solid relationship. Nevertheless it is important to mention that the small amount of results are actually not representative enough to use different statistic tests. So a larger amount of samples and tests could help providing larger sets of data and a more accurate statistical analysis.

Table 8: Summary of results (2)

	S_s*V (mg)	VAS (g)	F:M (mg/g)	Endogenous respiration (mg O₂/L/h)	HRT (min)	Duration (h)	T (°C)
Sample 1	3.84	27.120	0.14	± 3.5	27	± 2	17.92
Sample 2	6.58	66.985	0.10	± 8.5	36	± 5.5	17.46
Sample 3	6.88	28.698	0.24	± 9	27	± 1.5	17.79
Sample 4	7.27	73.141	0.10	± 8	34	± 3.3	16.41
Sample 4A	6.91	26.860	0.26	± 4.2	53	± 5.5	15.55
Sample 7	7.27	21.694	0.34	± 7.5	47	± 2	16.30
Sample 8	7.27	22.435	0.32	± 2.6	46	± 6.6	13.83

Diverse causes could be the origin for these fluctuating results. With the change from gravel media to soil media, a lot of difficulties were encountered. Different aspects on the respirometer were adjusted, but still various inaccuracies were present. Secondly, the soil composition has a possible influence on the tests. Little parts of roots, twigs or stones were removed from of the sample as much as possible, still some of these parts were present. This is also supposed to be the cause for more preferential flow paths.

More detailed info about the exact composition of the sample could help explain possible results as every sample was obtained from a different area of the wetland, leading to different circumstances and compositions. Important factors for this are the exact fraction of biomass in the soil, the exact composition and structure of the biomass, contaminants, trace elements... It would also be useful in future research, to determine the different parameters affecting the yield results and possibly find a correlation that way.

Other potential interferences during the tests could be the amount of acetate additions executed on one sample. However, no clear trend was observed in the results of different samples. The measuring-variances of the two DO-probes, preferential flow paths, hydraulic conductivities and the presence of different MO (including anaerobic and anoxic MO) could also disturb the results, together with the change of feeding and feeding load as the wetland is used to a higher amount of feeding with a more varied composition of components (compared to the sodium acetate substrate).

4.4.2 Growth yields

From the summarized values in table 7, the average Y_H is **0.776** mg COD/mg COD, but an outlier was detected at sample 8 which brings the average to **0.852** mg COD/mg COD when the outlier is excluded. The average Y_{STO} is **0.895** mg COD/mg COD. These values are much higher than the estimated values by Hoque et al. (2008) for the **SSAG** model. Compared to the estimation with the ASM3 model of Henze *et al.* (2000), a higher Y_H is measured with a similar Y_{STO} value. For the CWM1 of Langergraber *et al.* (2009) a Y_H of 0.63 g COD/g COD was proposed, which shows the biggest difference with the Y_H measured.

The lower values for Y_H rather than for Y_{STO} are consistent with research from the literature. Higher Y_H and Y_{STO} values are also obtained compared to a similar study by Ho (2018) with gravel media from lab-scale wetlands (with averages of $Y_H = 0.66 - 0.67$ and $Y_{STO} = 0.75 - 0.83$ mg COD/mg COD). The study of Pitzalis (2018) showed Y_H ranges of 0.52 – 0.72 g COD/g COD for a similar research with gravel media. Piscoeiro *et al.* (2017) measured Y_H ranges of 0.41 – 0.67 and for Y_{STO} : 0.75 – 0.83 g COD/g COD with gravel-based HSSF wetlands using a LSS-respirometer. This is lower than the obtained ranges of $Y_H = \mathbf{0.324 - 0.961}$ and $Y_{STO} = \mathbf{0.794 - 0.968}$ mg COD/mg COD.

The ranges from the soil based full-scale wetland show some similarities, but are more widely distributed (lower precision), with much higher values on average. A possible reason for the varying results could be due to the unequal distribution of aerobic and anaerobic/anoxic microorganisms. Regarding the wide distribution of yield values, high variances are observed throughout the complete wetland bed, which indicates that MO across a wetland bed could have different growth patterns.

Very high yield values were obtained during the tests. The most plausible explanation for these values would be the adsorption of substrate on the soil. This process, called biosorption, is a mechanism where different components (e.g. pollutants) bind with the porous surface and cell structure of the biomass. By adsorbing the added substrate, less oxygen is consumed during the tests which leads to these very high yield values. This overestimation of the growth yields is consistent with the work of Ho (2018) where gravel was used instead of soil. Gravel has a significantly less porous structure, which results in less adsorption and higher yield results. The adsorption-mechanism could also help explain some observations for the HRT as possible adsorption of the added NaCl could take place, but only with a small proportion.

The obtained results and proposed explanations above could be interesting to examine in future research and modelling studies. Notwithstanding no direct link is clear on how the growth patterns differ, evidence for a differing growth pattern is present. Yield values seem to be higher at the samples from the corners / side of the wetland, but it still varies too much to define a specific growth pattern throughout the bed. It also looks like a changing Y_H does not directly contribute to a varying Y_{STO} .

Differences between tests from the same sample showed little variances, with some explainable exceptions. Despite the absence of storage products at test 1 and 2 from sample 4 (figure 37 and figure 38) and test 2 from sample 7 (figure 43), growth yield coefficients were similar to results from the same sample with storage evidence (respectively $Y_H = 0.683$; 0.882 and 0.948 mg COD/mg COD).

As last, the results confirm the presence of the storage evidence which supports the perception that the SSAG model (or ASM3) is more appropriate as model to describe the determination of stoichiometric parameters for aerobic substrate biodegradation.

4.4.3 Respirogram types

Storage evidence was observed in 21 out of the 25 results divided over 12x type I (from 4 different samples), 6x type II (2 samples) and 7x type III (2 samples) respirograms. Comparable with previous researches, type I respirograms were the most common form. This includes the fast and sharp response of the microorganisms to the acetate addition (feast conditions), followed by a fast decrease of the OUR and ending with a slower oxygen consumption rate which represents the consumption of produced storage products (famine conditions). Based on earlier research together with this result, type I respirograms could possibly be assumed to be the standard respirogram. A standard respirogram for microorganisms as the natural reaction mechanism for aerobic substrate biodegradation in normal circumstances, i.e., with an intermittent feeding pattern in this case.

The second type of respirograms were perceived at two sample points of the wetland. Less knowledge is available about typical characteristics in order to obtain this type. With the data collected from the tests, no explicit indication is clear for properties of type II profiles. Because of the typical slow rise of the OUR during the feast period, there can be assumed this is caused by the slow migration of the substrate to the microorganisms (maybe caused by preferential flow paths / higher HRT). However, the slow rise could also be an indication of a longer time needed for the MO to adapt to new circumstances, i.e., aerobic conditions.

Secondly it could be caused by microorganisms used to slightly higher concentrations of COD with inconsistent loading rates and time of feeding. This could possibly explain the absence of storage products and the slow response to new substrate addition. More investigation is recommended to determine the detailed circumstances to create type II profiles. It may also act as an intermediate between type I and type III profiles.

Type III respirograms were observed clearly at sample points located at the inlet and outlet of the wetland (closest to the manholes where the water is guided to). This confirms the expectations that type III respirograms are connected to media subjected to higher loading rates on. Notwithstanding no evidence was found that higher growth yields are automatically guaranteed with these types of respirograms. For example, sample 8 revealed type III respirograms, but with a significant lower amount of microorganisms present in the sample and lower Y_H .

More tests should be performed, using multiple samples from the same area (intersections) at the wetland in order to investigate further characteristics from the wetland. At this point the variances on the test results are too large.

Chapter 5

Conclusion

5. Conclusion

5.1 Conclusion

5.2 Future research suggestions

5.1 Conclusion

During this research, stoichiometric parameters were measured successfully using an LSF-respirometer with sample from a soil based, full-scale operating HSSF constructed wetland. In order to create a working respirometry test, the respirometer was adjusted to counter the problems using soil media. The most important change was completed inside the box-reactor. A thin gravel layer at the inlet was inserted to create a water distribution layer. At the end of the box a second (larger) gravel layer was used as natural filter for dirt and turbidity and to lower the overall pressure drop. Compared to previous work, the transposition to tests with soil based samples caused the most difficulties. Promising results were obtained using the LSF-respirometer, but a second look needs to be done in order to reduce measuring errors and to ensure a proper test repeatability.

Samples from the wetlands were obtained with a sampling tube (provided with notches) which was inserted into the soil. Using a small shovel obstructing roots were cut. From this tube, soil samples were extracted by hand in order to avoid compression of the samples.

Samples from **10 points** at the wetland were collected (3x3 intersections + 1 extra point). At the middle centre of the wetland (sample 5), no tests were executed due to a highly dense structure of the soil. Results from the left hand side at the second and third row (sample 6 and 9) were neglected as quantitative results due to the high inaccuracy of the results.

Ranges for the hydraulic retention time were **22 – 53 min** and **22.970 – 131.343 g/L** for the volatile attached solids. Based on these results, a possible hypothesis was developed. Results showed lower values for the HRT and higher for the VAS at sample 2 (the inlet) and sample 4. This could indicate a possible preferential hydraulic pathway where influent from the inlet of the wetland, particularly flowing through the right hand side of the bed to the outlet (point 8). This with a much lower water flow through the left side. The (left) centre of the bed is assumed to be clogged. Contrary to the expectations similar results of the HRT and VAS were measured for all points at the third row of the wetland. These values were also comparable with some of the second row. It is not clear what caused the unexpected results for the last row (and sample point 6). Further investigation is needed in order to determine a possible obstruction by solids, excess of vegetation growth, efficiency of the BOD degradation and solid removal of the bed.

With the assumption that the measured HRT and VAS are correlated with certain occurrences inside the wetland bed, a few deviations probably need to be taken in account. The used soil inside the respirometer is subjected to different circumstances, which makes the results diverge from the real values inside the bed.

Results from a linear regression analysis were contradictory to the expectations. Only a few significant correlations were concluded (p -value < 0.05). Even with a statistically significant result, all results showed very weak relationships with adjusted R^2 -values less than 0.5.

Small correlations were observed for the maximum OUR peak height with the VAS (g/L) and the HRT. This is followed by a correlation for the level of endogenous respiration with the VAS, the HRT and the duration of the test. Also a relationship between the temperature and the tests duration, maximum OUR peak and HRT is detected. These varying results with a high variation could be the result of many inaccuracies during the measurement and the lack of information about the exact soil composition or exact amount and species of microorganisms (biomass).

In order to perform more accurate statistical analysis, more samples should be obtained and a larger range of tests would need to provide more data. The small amount of results are, in this case, probably not enough to get to quantitative conclusions.

Different yield coefficients were calculated with a wide distribution of the yields over the different sample points. Ranges for Y_H and Y_{STO} are respectively **0.324 – 0.961** and **0.794 – 0.968** mg COD/mg COD with an average $Y_H = 0.852$ mg COD/mg COD (0.776 with outlier) and $Y_{STO} = 0.895$ mg COD/mg COD. This is consistent with the literature where lower values for Y_H were obtained comparing to Y_{STO} . Nevertheless, the measured growth yields are higher compared to the more precise yields from gravel based, lab-scale wetlands. Results from tests with the same samples were obtained with small variances (good repeatability).

A highly assumable reason for the extremely high yield values is the adsorption of substrate on to the soil. This is called biosorption and would lead to a lower oxygen consumption as substrate is adsorbed without being oxidized.

From all 25 respirograms **12x type I**, **7x type II** and **6x type III** respirograms were obtained as explained by PISOEIRO *et al.* (2017). Storage was observed in **21 out of 25** results. These results showed similarities with previous researches with type I as most common (standard) profile and only a few type II and III profiles. Type II is probably more favourable in areas with a lower hydraulic conductivity or with higher, but fluctuating loading rates and times of feeding. It could also be due to a longer time for the MO to adjust to new circumstances. Type III is assumed to occur with microorganisms used to a high loading rate. However it could also act as an intermediate between type I and III. The different types of obtained respirograms do not seem to influence the yield values.

Evidence for the storage mechanism was sufficient present throughout the tests. Together with the obtained data, the ASM3 and SSAG models seem to be appropriate models to describe the determination of stoichiometric parameters for aerobic substrate biodegradation. Also the varying yield results indicate different growth patterns of microorganisms across the wetland bed.

5.2 Future research suggestions

In earlier research including of Ho (2018) and Pitzalis (2018) the use of respirometry to determine stoichiometric parameters from lab-scale HSSF constructed wetlands proved to be successful. When implementing samples from soil-based wetlands into this method, results were obtained with wide deviations. Moreover a lot of difficulties were encountered regarding the change of media from gravel to soil. Therefore further elaboration is recommended to calibrate an optimal operating procedure using LSF respirometers for respirometry of soil-based media from HSSF wetlands. The investigation of the detailed soil composition could be useful to interpret results.

The used respirometer was easy to assemble with standard lab-equipment, but together with the development of respirometry procedure, the set-up of a more robust respirometer could help to obtain more precise results.

With the results for the types of OUR-profiles as explained by PISOEIRO *et al.* (2017), more comprehensive possible explanations were developed for these different types and the relation with behaviour of the MO. Further research would be suggested to get a better view on the different circumstances in different places at the wetland and the specific performance of MO with it. Also a larger amount of tests should be performed with multiple samples from the same area of the wetland in order to achieve a more reliable result. A hydraulic conductivity test *in-situ* would be recommended to confirm possible areas of clogging. But most importantly, a method should be calibrated to determine the specific soil composition and especially the exact amount of biomass present in the soil. Next to this, the inhibition of substrate addition on to the soil needs to be found and use, or a method to determine the total adsorption capacity so this could be used as a correction factor.

References

- Andreottola, G., Oliveira, E., Foladori, P., Peterlini, R., Ziglio, G., 2007. Respirometric techniques for assessment of biological kinetics in constructed wetland. *Water Sci. Technol.* 56, 255–261. <https://doi.org/10.2166/wst.2007.512>
- Bonner, R., Aylward, L., Kappelmeyer, U., Sheridan, C., 2017. A comparison of three different residence time distribution modelling methodologies for horizontal subsurface flow constructed wetlands. *Ecol. Eng.* 99, 99–113. <https://doi.org/10.1016/j.ecoleng.2016.11.024>
- Boone, R., 2016. De selectieve respons van heterotrofe waterzuiveringsprocessen bij de overgang van mesofiele naar thermofiele temperaturen. Ghent University.
- Brdjanovic, D., Meijer, S.C.F., Lopez-Vazquez, C.M., Hooijmans, C.M., van Loosdrecht, M.C.M., 2015. *Applications of Activated Sludge Models*. IWA Publishing.
- Brix, H., 2003. Plants used in constructed wetlands and their functions. 1 st Int. Semin. Use Aquat. Macrophytes wastewater Treat. Constr. Wetl. 1, 30. <https://doi.org/10.1016/j.ejphar.2014.05.01.3>
- Chambers, R.M., Meyerson, L.A., Saltonstall, K., 1999. Expansion of *Phragmites australis* into tidal wetlands of North America. *Aquat. Bot.* 64, 261–273. [https://doi.org/10.1016/S0304-3770\(99\)00055-8](https://doi.org/10.1016/S0304-3770(99)00055-8)
- Compo Expert Benelux nv, n.d. Werking van DMPP. compo-expert.com 2.
- Decamp, O., 1996. The microbial ecology of the root zone method of wastewater treatment. Leicester.
- Dizdaroglu-Risvanoglu, G., Karahan, Ö., Cokgor, E.U., Orhon, D., Van Loosdrecht, M.C.M., 2007. Substrate storage concepts in modeling activated sludge systems for tannery wastewaters. *J. Environ. Sci. Heal. - Part A Toxic/Hazardous Subst. Environ. Eng.* 42, 2159–2166. <https://doi.org/10.1080/10934520701629658>
- Dotro, G., Molle, P., Nivala, J., Puigagut, J., Stein, O., Günter, L., Marcos, von S., 2017. *Biological wastewater treatment series. Volume 7: Treatment wetlands, First edit.* ed. IWA Publishing, London. <https://doi.org/10.2166/9781780408774>
- EPA, 2001. METHOD 1684 Total , Fixed , and Volatile Solids in Water , Solids , and Biosolids Draft January 2001 U . S . Environmental Protection Agency Office of Water Office of Science and Technology Engineering and Analysis Division (4303) 1–13.
- Galvão, A., 2017. *RESPIROMETRY PRINCIPLES AND APLICATIONS*, Instituto Superior Técnico. Instituto Superior Técnico, Lisbon.
- Galvão, A., Matos, J., 2012. Response of horizontal sub-surface flow constructed wetlands to sudden organic load changes. *Ecol. Eng.* 49, 123–129. <https://doi.org/10.1016/j.ecoleng.2012.08.033>
- Gernaey, A.K., Petersen, B., Ottoy, J.P., Vanrolleghem, P., 2001. Activated sludge monitoring with combined respirometric-titrimetric measurements. *Water Res.* 35, 1280–1294.

[https://doi.org/10.1016/S0043-1354\(00\)00366-3](https://doi.org/10.1016/S0043-1354(00)00366-3)

- Hao, X. Di, Wang, Q.L., Zhu, J.Y., Van Loosdrecht, M.C.M., 2010. Microbiological endogenous processes in biological wastewater treatment systems. *Crit. Rev. Environ. Sci. Technol.* 40, 239–265. <https://doi.org/10.1080/10643380802278901>
- Harrison, J., 2016. Phragmites invasion: Detrimental or beneficial? *delmarvanow.com* 1.
- Henze, M., Gujer, W., Mino, T., Van Loosdrecht, M.C.M., 2000. Activated Sludge Models ASM1, ASM2, ASM2d and ASM, 2nd ed, Scientific and Technical Report series. IWA Publishing, London.
- Ho, S.P., 2018. Determining stoichiometric parameters in macrophyte beds with a fixed biomass respirometer *Engenharia do Ambiente*. ULisboa.
- Hoque, M.A., Aravinthan, V., Pradhan, N.M., 2008. Evaluation of simultaneous storage and growth model to explain aerobic biodegradation of acetate *Evaluation of Simultaneous Storage and Growth Model to explain Aerobic Biodegradation of Acetate*. *Res. J. Biotechnol.* 11.
- Interpro, 2018. Ammonia monooxygenase/particulate methane monooxygenase, subunit B [WWW Document]. *ebi.ac.uk*. URL <https://www.ebi.ac.uk/interpro/entry/IPR006833>
- IWA, 2016. Water and sanitation services [WWW Document]. *Int. Water Assoc.* URL <http://www.iwa-network.org/programs/water-and-sanitation-services/>
- Jeppsson, U., 1996. A General Description of the Activated Sludge Model No . 1 (ASM1). Components 1, 1–16. <https://doi.org/10.1007/s00540-017-2318-2>
- Kadlec, R.H., Wallace, S.D., 2009. *Treatment Wetlands Second Edition*. Taylor & Francis Group LLC, Boca Raton.
- Langergraber, G., Rousseau, D.P.L., García, J., Mena, J., 2009. CWM1: A general model to describe biokinetic processes in subsurface flow constructed wetlands. *Water Sci. Technol.* 59, 1687–1697. <https://doi.org/10.2166/wst.2009.131>
- Nave, B., Dickhaut, J., Sisay, M.T., Wissemeier, A., Zerulla, W., Ebenhoech, J., Weigelt, W., 2017. Nitrification Inhibitors. *ipni.net* 15030.
- O'Dell, J.W., 1993. Method 410.4, Revision 2.0: The Determination of Chemical Oxygen Demand by Semi-Automated Colorimetry. Cincinnati, Ohio.
- Ortigara, A.R.C., Foladori, P., Andreottola, G., 2011. Kinetics of heterotrophic biomass and storage mechanism in wetland cores measured by respirometry. *Water Sci. Technol.* 64, 409–415. <https://doi.org/10.2166/wst.2011.547>
- Pisoeiro, J., Galvão, A., Pinheiro, H.M., Ferreira, F., Matos, J., 2017. Determining stoichiometric parameters of detached biomass from a HSSF-CW using respirometry. *Ecol. Eng.* 98, 388–393. <https://doi.org/10.1016/j.ecoleng.2016.07.003>
- Pitzalis, T., 2018. Respirometry techniques for the determination of kinetic and stoichiometric parameters in HSSF-CW. UNIVERSITÀ DEGLI STUDI DI CAGLIARI.

- Rousseau, D., 2017. Ecotechniek - deel 2, in: MACRO-ECOLOGIE En ECOTECHNIEK. Kortrijk, p. 53.
- Scholz, M., 2016. Activated Sludge Processes. *Wetl. Water Pollut. Control* 91–105. <https://doi.org/10.1016/B978-0-444-63607-2.00015-0>
- Sin, G., Guisasola, A., De Pauw, D.J.W., Baeza, J.A., Carrera, J., Vanrolleghem, P.A., 2005. A new approach for modelling simultaneous storage and growth processes for activated sludge systems under aerobic conditions. *Biotechnol. Bioeng.* 14. <https://doi.org/10.1002/bit.20741>
- Spanjers, H., Vanrolleghem, P.A., Ekama, G.A., 2016. 3 Respirometry, in: EXPERIMENTAL METHODS IN WASTEWATER TREATMENT. IWA Publishing, London, p. 44.
- Tilley, E., Ulrich, L., Lüthi, C., Reymond, P., Zurbrügg, C., 2014. Compendium of Sanitation Systems and Technologies. *Development* 158. <https://doi.org/SAN-12>
- Van Hulle, S., 2016. Watertechnologie. UGent Campus Kortrijk, Kortrijk.
- Van Loosdrecht, M.C.M., Nielsen, P.H., Lopez-Vazquez, C.M., Brdjanovic, D., 2016. *Experimental Methods in Wastewater Treatment*, Illustrate. ed. IWA Publishing.
- Vanrolleghem, P.A., 2002. Principles of respirometry in activated sludge wastewater treatment. *Dep. Appl. Math. biometrics Process Control . Belgium* 32, 1–19.
- Vymazal, J., 2005. Horizontal sub-surface flow and hybrid constructed wetlands systems for wastewater treatment. *Ecol. Eng.* 25, 478–490. <https://doi.org/10.1016/j.ecoleng.2005.07.010>
- Weiss, N.A., 2016. *Introductory Statistics*, 9th Edition., 9th ed. Pearson (Addison-Wesley), Arizona.
- WHO, 2018. Drinking-water [WWW Document]. World Health Organ. URL <https://www.who.int/en/news-room/fact-sheets/detail/drinking-water> (accessed 1.20.19).
- Windsor, C., Steinbach, A., Lockwood, A., Mooney, R.J., 2012. In-Situ ® Optical RDO ® Methods for Dissolved Oxygen Measurements Outperform Traditional Methods.
- Zacherl, B., Amberger, A., 1990. Effect of the nitrification inhibitors dicyandiamide, nitrapyrin and thiourea on *Nitrosomonas europaea*. *Fertil. Res.* 22, 37–44. <https://doi.org/10.1007/BF01054805>

Appendices

Appendix A: SSAG stoichiometric- and kinetic parameters for respirometry

Table 9: A summary of the stoichiometric- and kinetic parameters for respirometry according to the SSAG model (Hoque et al., 2008)

Process	X_H	X_{STO}	S_S	S_O	Kinetics
Formation of X_{STO}		1	$-1/Y_{STO}$	$-(1-Y_{STO})/Y_{STO}$	$(1 - e^{-t/\tau})k_{STO}M_S X_H$
Aerobic growth on S_S	1		$-1/Y_{H,S}$	$-(1-Y_{H,S})/Y_{H,S}$	$(1 - e^{-t/\tau})\mu_{max,S}M_S X_H$
Aerobic growth on X_{STO}	1	$-1/Y_{H,STO}$		$-(1-Y_{H,STO})/Y_{H,STO}$	$\mu_{maxSTO} \left(\frac{(X_{STO}/X_H)^2}{K_2 + K_1(X_{STO}/X_H)} \right) \left(\frac{K_S}{S_S + K_S} \right) X_H$
Endogenous respiration	-1			$-(1-f_{XT})$	$b_H X_H$
X_{STO} respiration		-1		-1	$b_{STO} X_{STO}$

Appendix B: Results for the constructed wetland influent and effluent concentrations

Table 10: Constructed wetland influent and effluent concentrations (2002 - 2005)

Physical and chemical parameters		16/10/2002		19/03/2003		4/11/2003		16/03/2005		Emission limit
		IN	OUT	IN	OUT	IN	OUT	IN	OUT	
pH	(-)	7.1	6.7	6.8	7.2	7.5	7.3	7.8	7.3	6.5-0-9.5
BOD ₅	(mg/L O ₂)	80	<25	160	100	96	5	88	4	40
COD	(mg/L O ₂)	174	<50	370	210	390	120	450	76	150
Total Phosphorus	(mg/L P)	3	2	2	2	0.8	0.55	6.2	4.9	10
Total Nitrogen	(mg/L N)	28	14	115	104	50	6.4	76	26	15
Oils and Greases	(mg/L)	15	<10	-	-	-	-	9.5	<0.1	15
TSS	(mg/L)	26	26	118	56	119	16.4	10	<2	60
Microbiological parameters		16/10/2002		19/03/2003		4/11/2003		16/03/2005		
		IN	OUT	IN	OUT	IN	OUT	IN	OUT	
Total coliforms	(NMP/100ml)	7900000	80000	100000	24000	5850000	616	>160000	140	
Faecal coliforms	(NMP/100ml)	-	-	-	-	-	-	350	27	
Streptococcus	(NMP/100ml)	-	-	-	-	-	-	160000	130	
Helminth Eggs	(-)	-	-	-	-	-	-	-	-	
Salmonella	(Em 1000ml)	-	-	-	-	-	-	Negative	Negative	

Appendix C: HRT-profiles for every sample

